Faculty of Mechanical Engineering

dr. Jure Ravnik,

professor of power, process and environmental engineering

Recent results in modelling and simulation of particle laden flows

Laboratory for transport phenomena in solids and fluids

Acknowledgements:
- Matjaž Hriberšek
- Paul Steinmann
- Yan Cui
- Mitja Štrakl
- Jana Wedel
- František Lizal

Contact:
- ***jure.ravnik@um.si***
- ***http://jure.ravnik.si***
- ***@JureRavnik***

University of Maribor

2023

Introduction

- Multiphase flows
  - Dispersed flows with particles
- Numerical approach
  - Euler-Lagrange framework
    - Euler: Carrier fluid phase
    - Lagrange: Particulate phase
  - Point-particle method
    - Particle size << Kolmogorov length scale

      $d_p \ll \eta_K \quad St_p \ll 1$
    - Flow around the particle → viscous regime

      $Re_p \ll 1 \quad Re_G \ll Re_p$

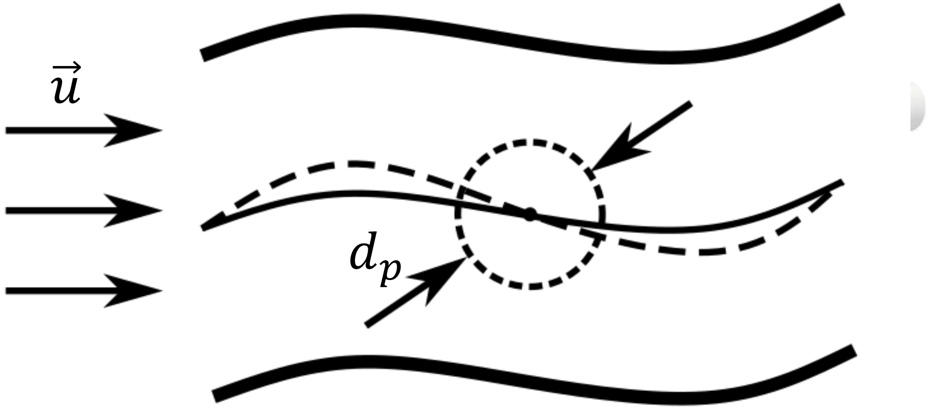

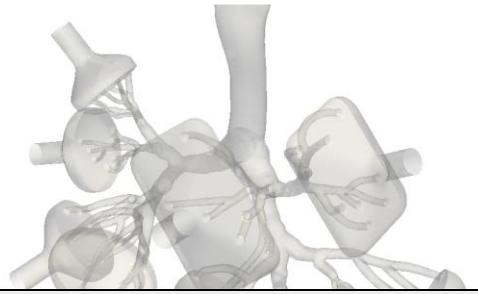

⇒ Particle-Fluid interaction is modeled

Motivation

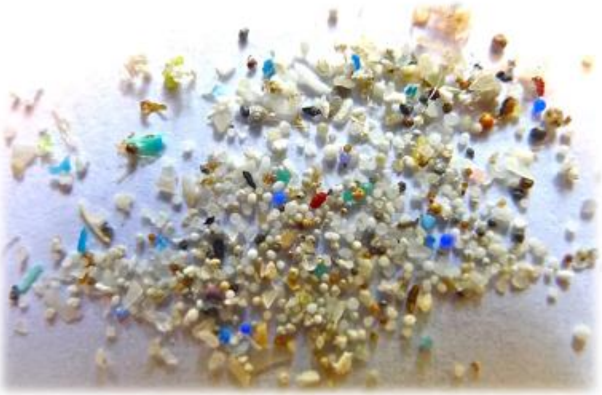

Oregon State University, CC BY-SA 2.0, via Wikimedia Commons

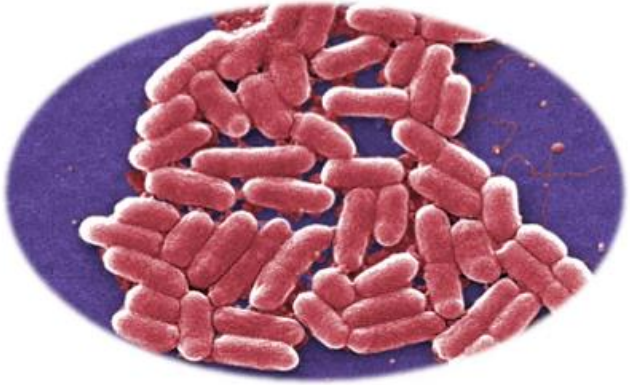

James Joel, 2006, National Escherichia, Shigella, Vibrio Reference Unit at CDC *2

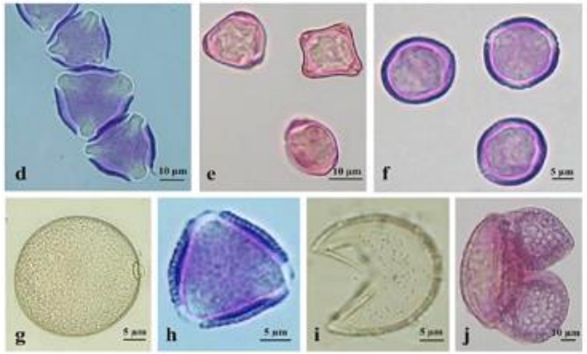

Denisow, B. and Weryszko-Chmielewska, E. Photo: Irene Câmara Camacho., CC BY-SA 4.0, via Wikimedia Commons

Particles in fluids

Picture of James Gathany, Brian Judd, USCDCP from Pixino

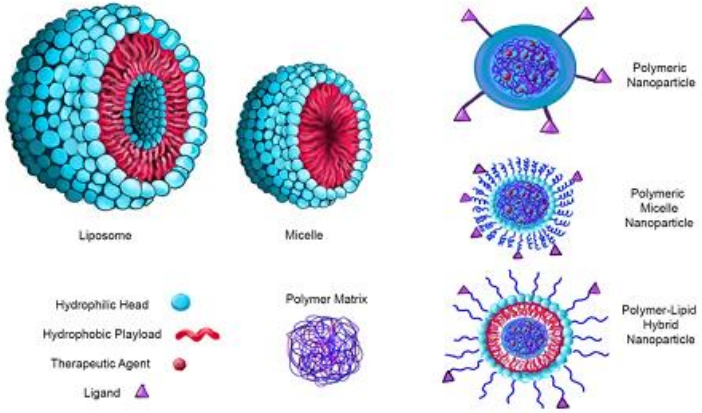

WolfpackBME, CC BY-SA 4.0, via Wikimedia Commons

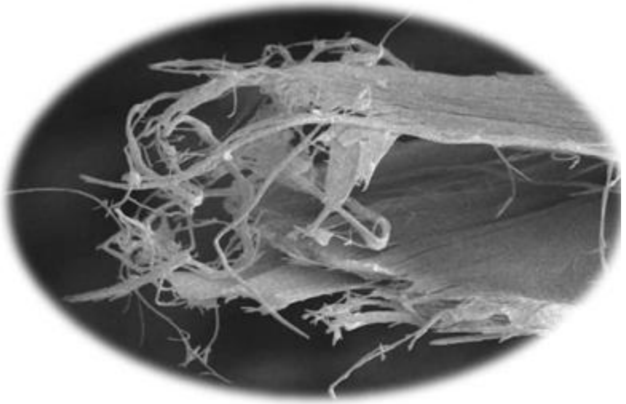

Liangtai Lin, CC BY 2.0, via Wikimedia Commons

Motivation

- we are constantly exposed to airborne pollutants

GRAIN OF SAND
90 μm >

GRAIN OF SALT
60 μm >

Pollen
5 - 20 μm >

Visibility limits for the naked eye
$\approx 10 - 40\ \mu m$

RESPIRATORY DROPLETS
5 - 10 μm >

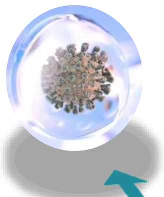

can carry smaller particles such as viruses

mostly non-spherical

Dust Particles
PM2.5 2.5 μm >

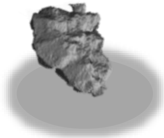

Bacterium
1- 3 μm >

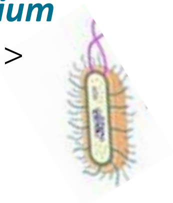

Wildfire smoke
0.4-0.7 μm

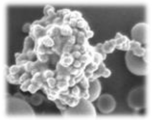

Corona virus
0.1- 0.5 μm >

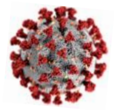

Wildfire smoke can persit in the air for several days and even months

Superellipsoid formulation

$$E(r') = \left[\left[\frac{x'}{a}\right]^{2/\epsilon_2} + \left[\frac{y'}{b}\right]^{2/\epsilon_2}\right]^{\epsilon_2/\epsilon_1} + \left[\frac{z'}{c}\right]^{2/\epsilon_1}$$

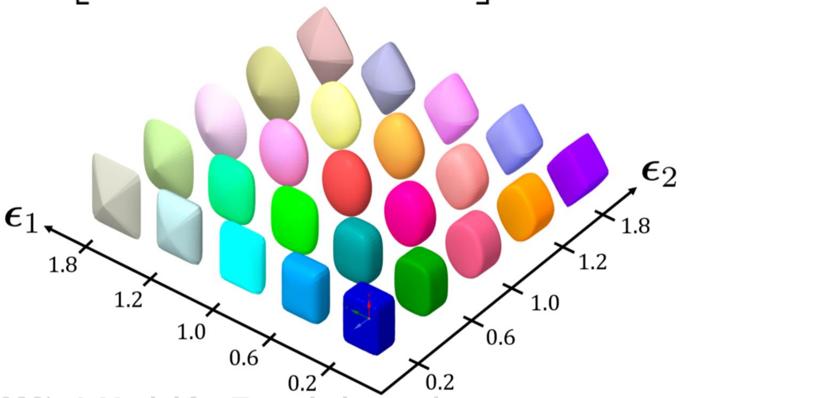

Štrakl, M., Hriberšek, M., Wedel, J., Steinmann, P., Ravnik, J. (2022). **A Model for Translation and Rotation Resistance Tensors for Superellipsoidal Particles in Stokes Flow.** J. Mar. Sci. Eng. 2022, 10, 369. doi:10.3390/jmse10030369

Research topics covered

- Spherical particles:
  - Application to tracking of aerosol in human respiratory tract
- Superellipsoidal particles:
  - Drag force and torque modelling
  - Collision modelling

Motivation - pathways of Covid-19 transmission

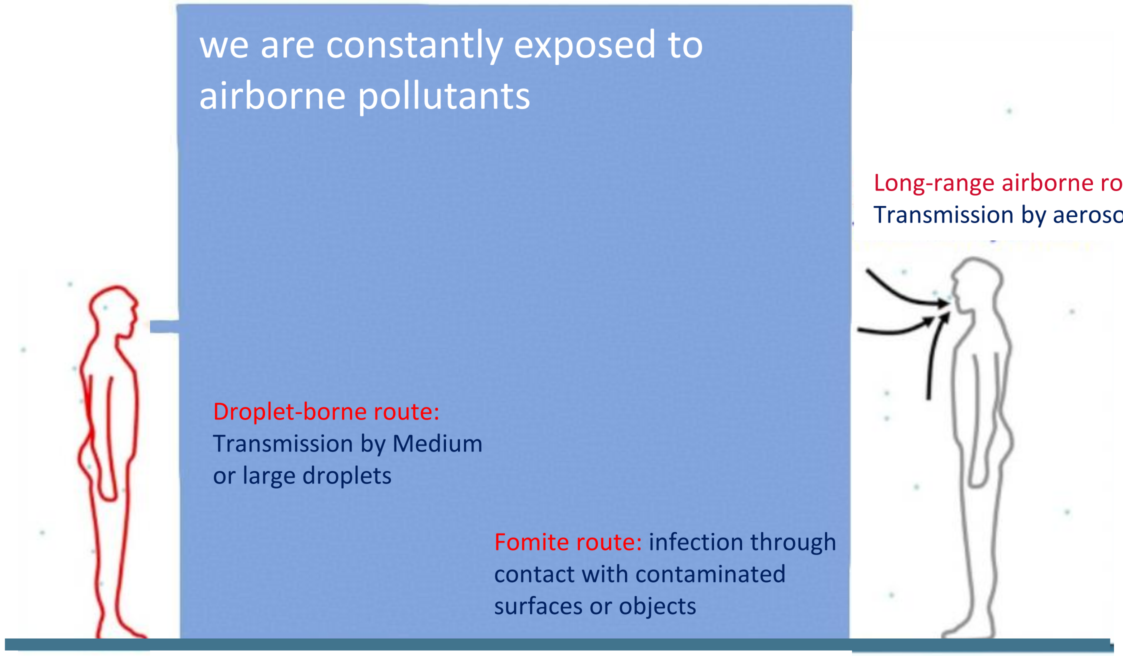

- dp $> 100\ \mu m$: Fast deposition due to the domination of gravitational force
- Medium droplets between $5\ \mu m$ and $100\ \mu m$
- dp $< 5\ \mu m$: Small droplet nuclei or aerosols - Responsible for airborne transmission

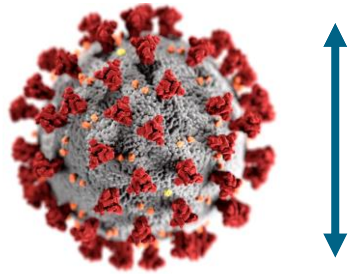

70–90 nm [1]

Giaimo C (1 April 2020). "The Spiky Blob Seen Around the World". The New York Times.

Realistic human lung replicas

- Resolved until 7-10th level of bifurcation (LoBF)
- Inhalation: $\dot{V}_e = [7.5, 15, 30]\,\frac{l}{min}$

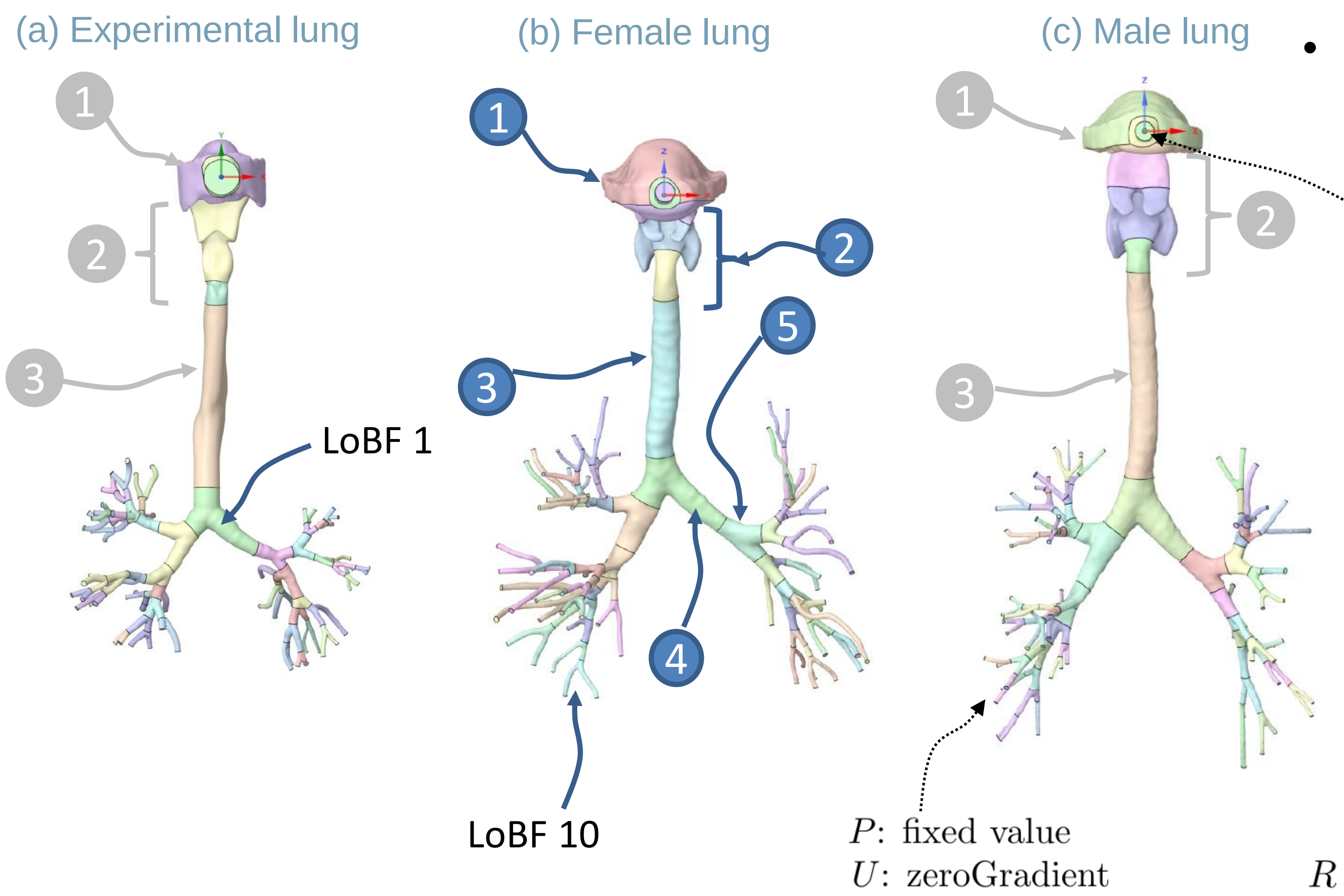

Airway	Experimental lung	Female Lung	Male Lung
Cells	8.3 Mio	9.7 Mio	8.5 Mio
Boundary layers	5	5	5
Near wall distance	$y^+ \approx 1$	$y^+ \approx 1$	$y^+ \approx 1$
R [Pa s/l]	22.91	50.492	47.08

$R = \Delta p / \dot{V}_e$

Methodology

Flow field equations

- The flow field is solved in an Eulerian framework with OpenFOAM® (uses FVM)
- The governing incompressible RANS equations are:

$$\mathrm{d_t}(\rho_f \bar{\boldsymbol{u}}) + \mathrm{div}(\rho_f \bar{\boldsymbol{u}} \otimes \bar{\boldsymbol{u}} + \boldsymbol{\tau}^{\mathrm{RANS}}) = -\mathrm{grad}\bar{p} + \mathrm{div}\bar{\boldsymbol{\tau}} + \bar{\boldsymbol{f}}_D \quad \text{and} \quad \mathrm{div}\bar{\boldsymbol{u}} = 0$$

Note that: $\boldsymbol{u} = \bar{\boldsymbol{u}} + \boldsymbol{u}'$

$$\boldsymbol{\tau}^{\mathrm{RANS}} := \rho_f \boldsymbol{u}'_i \otimes \boldsymbol{u}'_j \qquad \bar{\boldsymbol{\tau}} := \mu\, \mathrm{grad}^{\mathrm{SYM}} \bar{\boldsymbol{u}}$$

Lagrangian particle formulation

- Maxey-Riley equation

$$\boldsymbol{a}^* = \frac{d\boldsymbol{v}^*}{dt^*} = \frac{A}{St}\left[\boldsymbol{v}_s^* + \frac{c}{3d_{eq}}\boldsymbol{K}\cdot[\boldsymbol{u}^* - \boldsymbol{v}^*]\right] + \frac{3}{2}R\frac{\partial \boldsymbol{u}^*}{\partial t^*} + R\left[\left[\boldsymbol{u}^* + \frac{1}{2}\boldsymbol{v}^*\right]\cdot\boldsymbol{\nabla}\right]\boldsymbol{u}^*$$

$$A = \frac{\rho_p}{\rho_p + 0.5\rho_f}$$

$$St = \frac{1}{18}\frac{\rho_p}{\rho_f}\frac{d_{eq}^2}{\nu}\frac{u_0}{L_0}$$

$$\boldsymbol{v}_s^* = \frac{1}{18}\frac{d_{eq}^2}{\nu u_0}\left[\frac{\rho_p}{\rho_f} - 1\right]\boldsymbol{g}$$

$$R = \frac{\rho_f}{\rho_p + 0.5\rho_f}$$

neglegible if:

- $\rho_p \gg \rho_f$
- $St \ll 1$

Particles

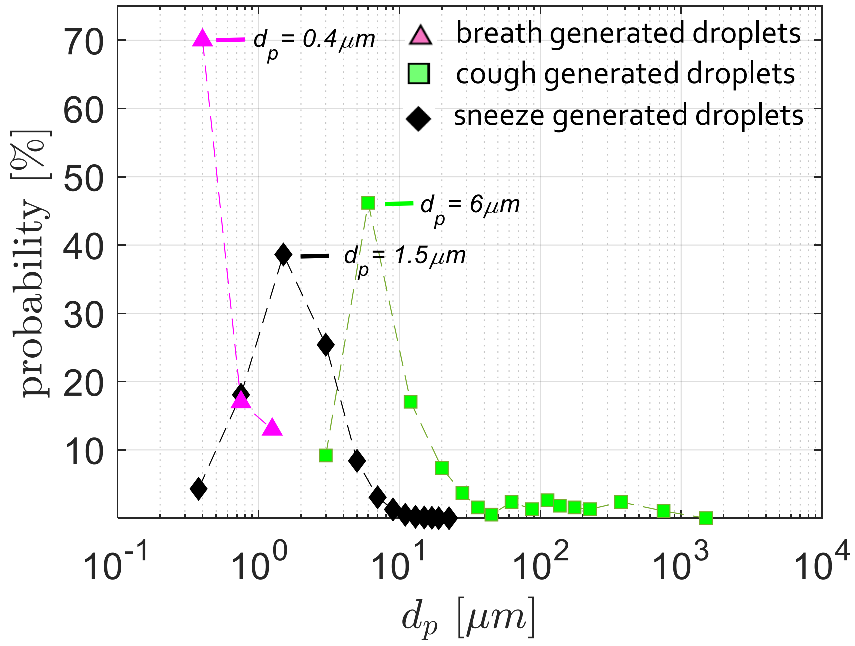

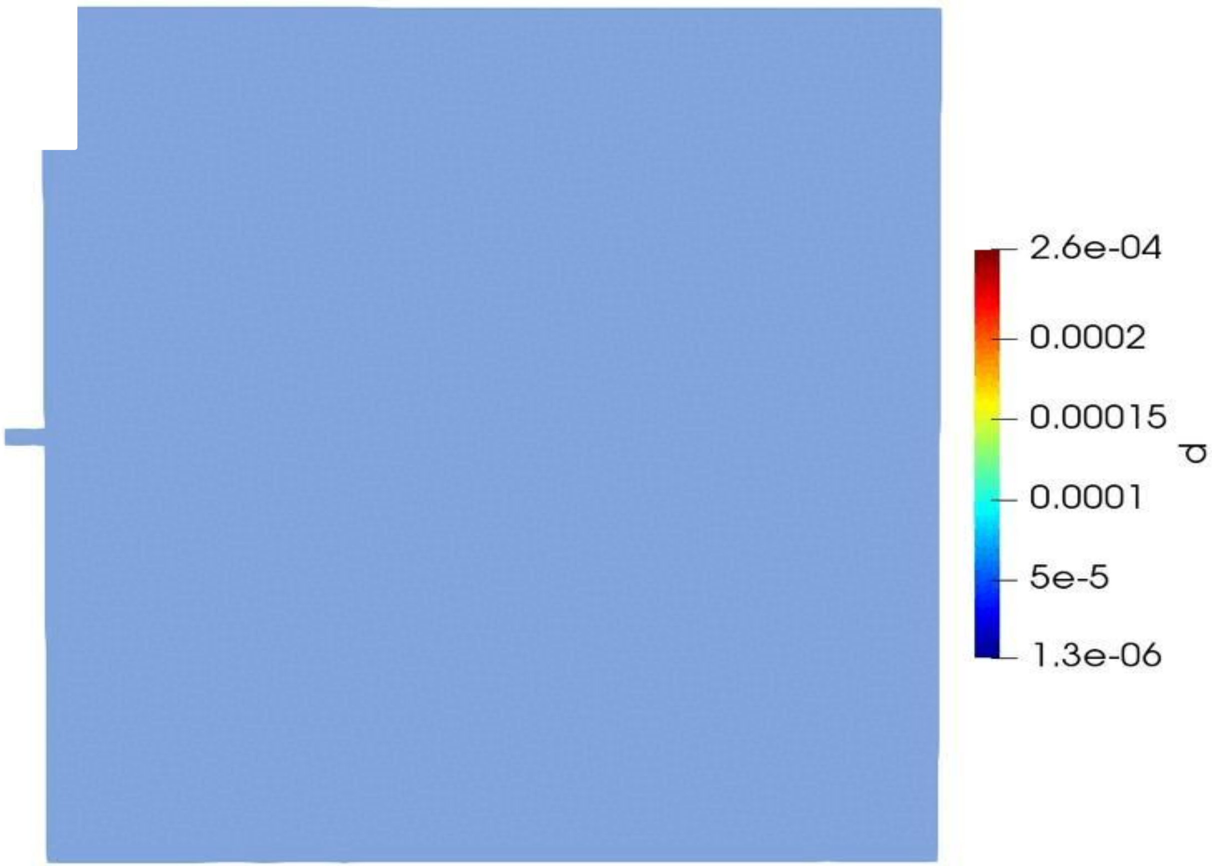

- **10^5 spherical** and **rigid** particles, ρ_p =1704kg/m3
- cough, sneeze and breath generated particles
- touch & stick wall interaction
- **drag**, **gravity and buoyancy** $(\rho_p \gg \rho_f, St \ll 1)$
- turbulent dispersion: Continuous random walk
- initial particle velocity is set to local flow-velocity

Limitations

- **dilute flow** allowing for one-way coupling of particles and fluid,
- assumption of **isotropic turbulence** (turbulent dispersion model: *StochasticDispersionRAS*) and k-ω-SST / k-ω-SST DES RANS turbulence approach,
- sufficiently small aerosols: surface tension strong enough → small spherical rigid particles,
- we study **aerosol deposition in selected lung regions rather than precise deposition** locations,
- particle volume fractions is well below 10^{-6} (suggested limit for one-way coup. by Elghobashi (1994)),
- majority of d_p (average sizes: $0.3\ \mu m$ (speaking), $1.5\ \mu m$ (cough), $6\mu m$ (sneeze)) are smaller than $\eta_k = R_e^{-3/4} D_{inlet}$ → their impact on the turbulence modulation is small (see Crowe 2000),

→ Combining these statements, we consider **RANS with one-way coupling as appropriate** in the scope of the present application.

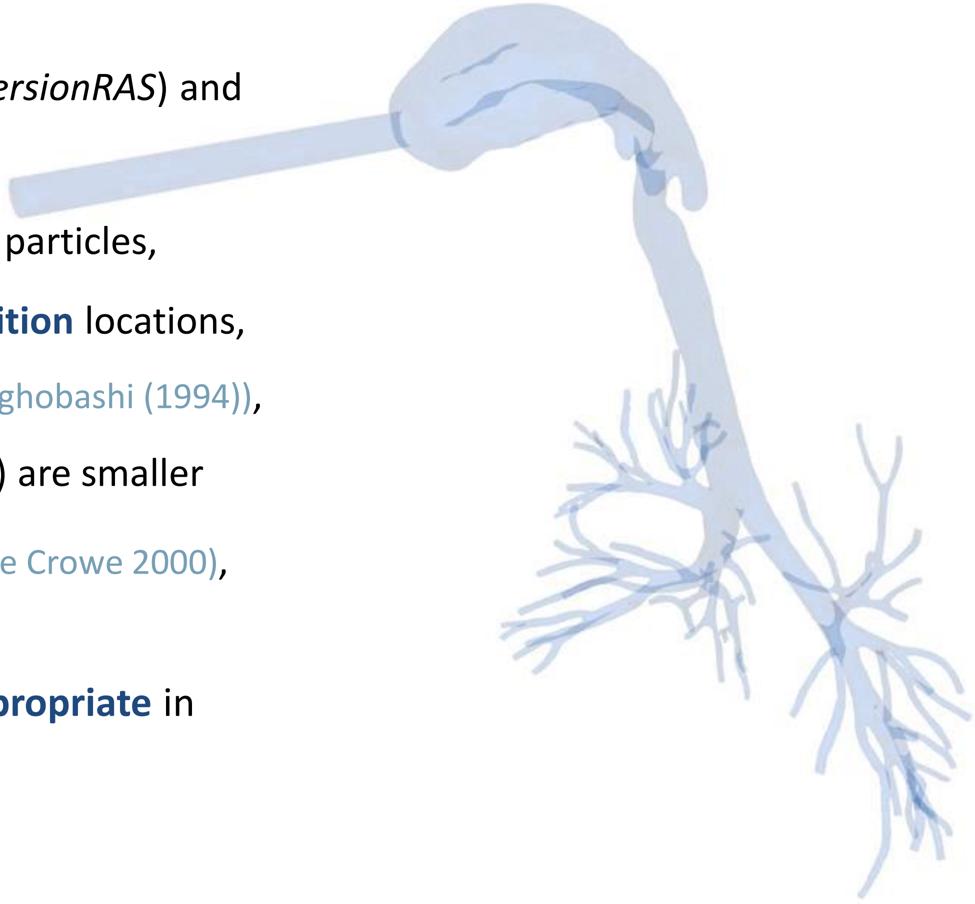

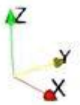

Flow simulation results

- Velocity distribution in central plane

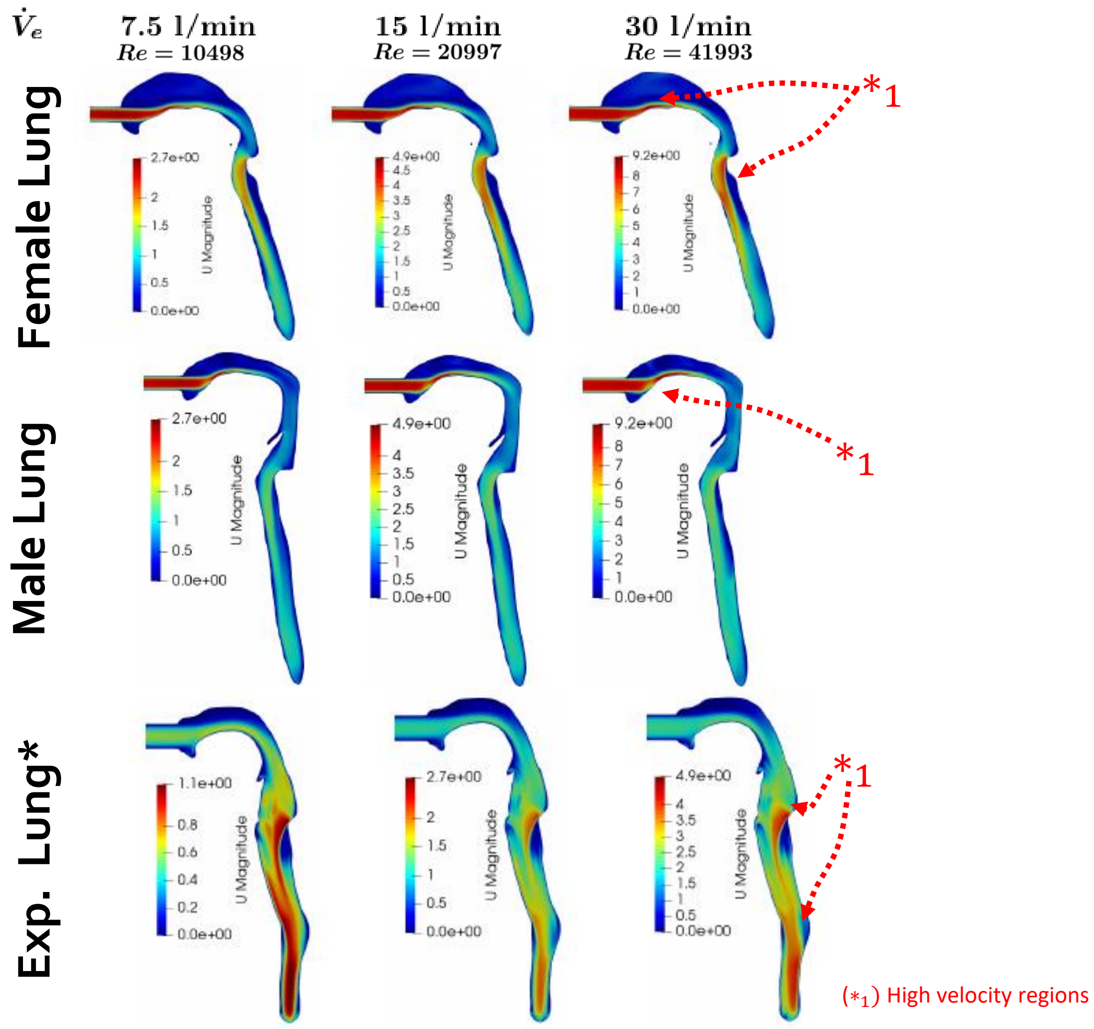

- Turbulent kinetic energy distribution in central plane

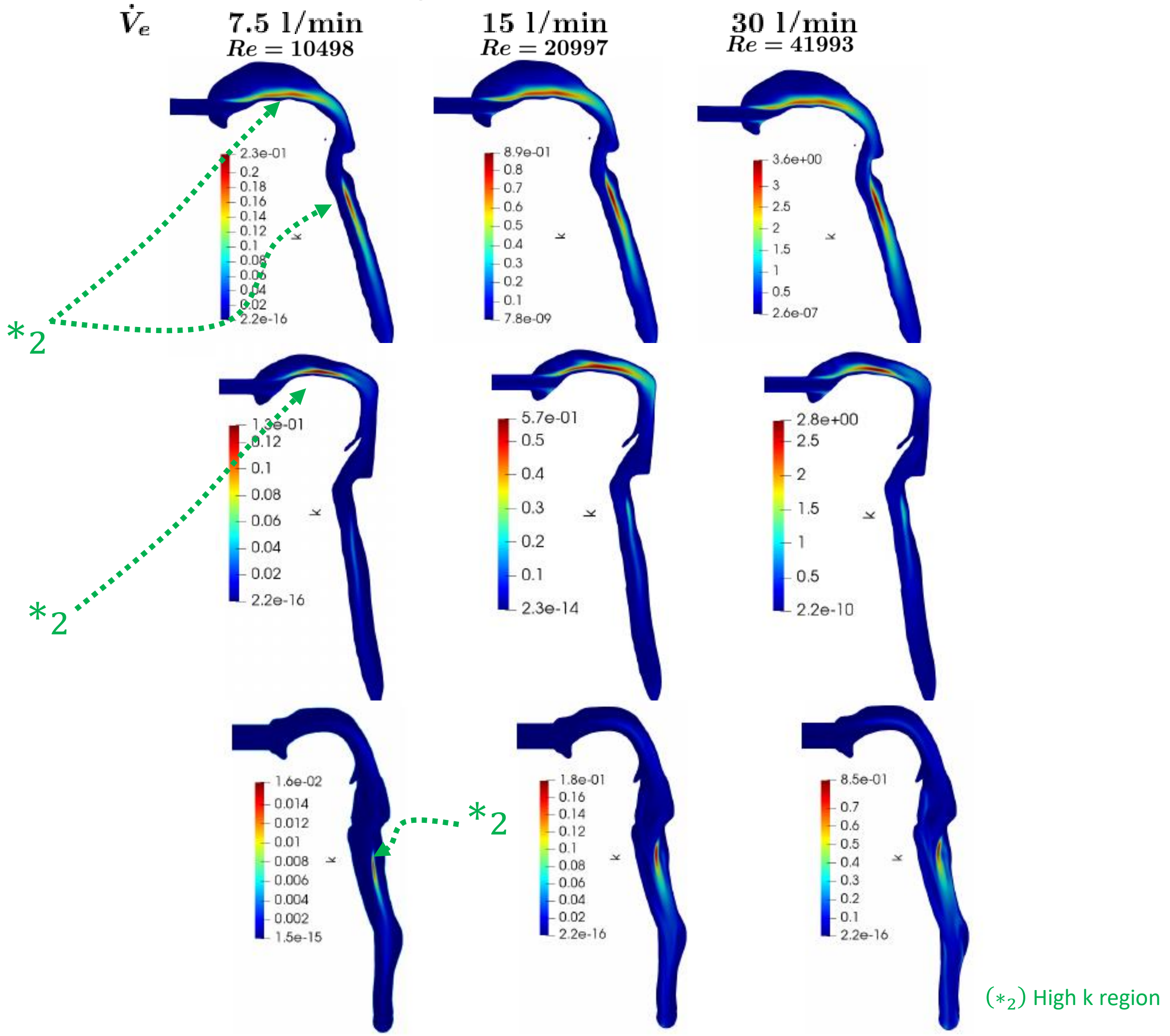

*Note the different Reynolds numbers due to different inlet diameter of experimental lung ($R_{e,exp} = 1/2\ R_e$)

Deposition

- steady state inhalation
- study volumetric deposition efficiency (DE)
- particles produced by breathing, coughing, or sneezing
- 10^5 inhaled particles

Female Lung:

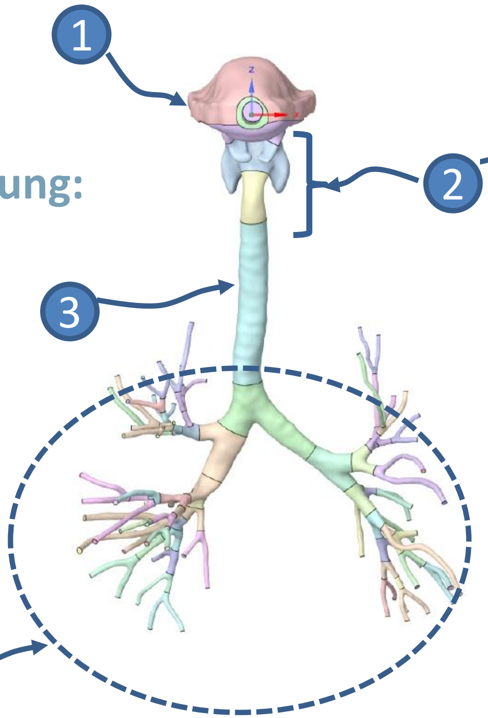

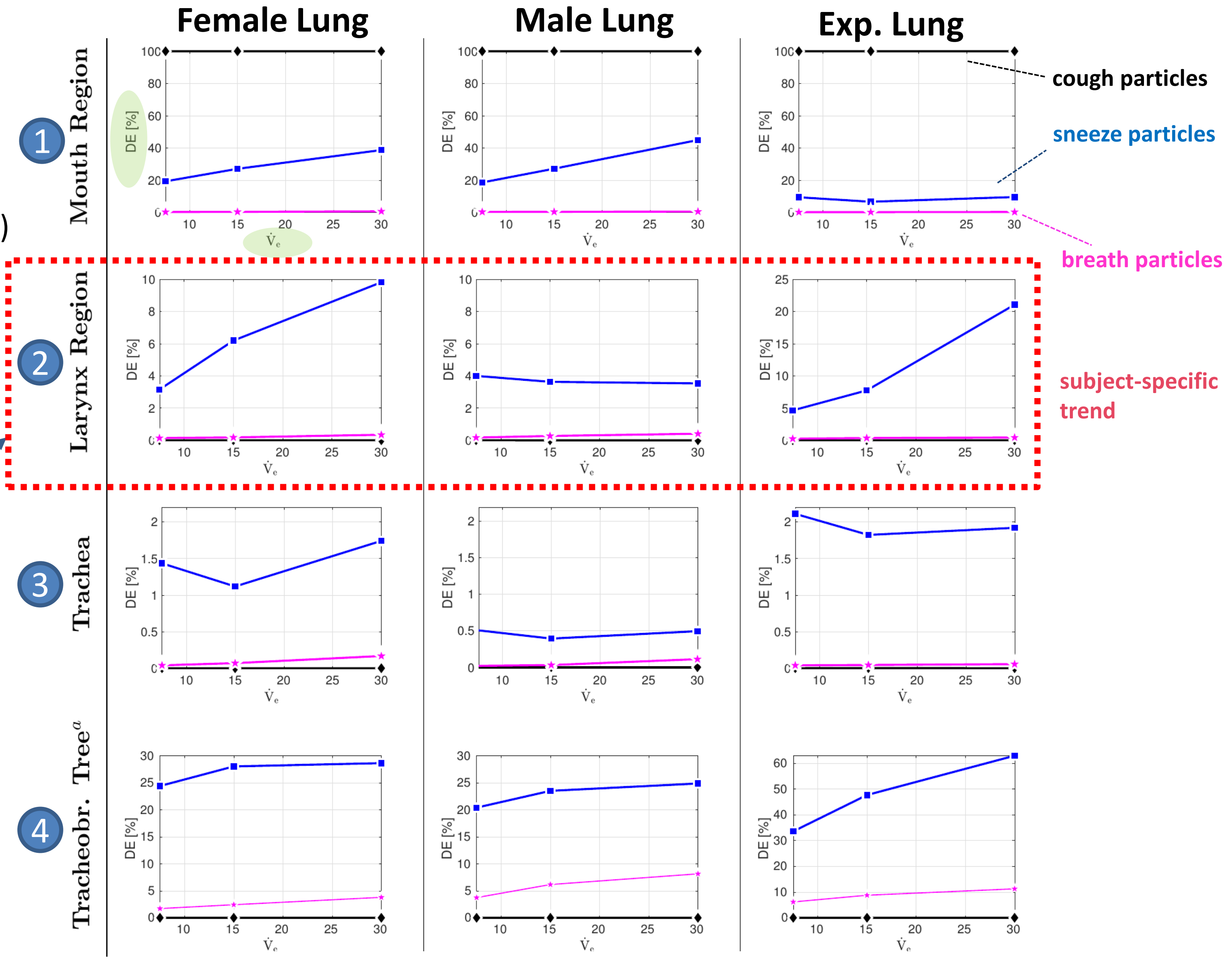

Volumetric deposition fraction across three exercising levels; ◆ coughing droplets, ■ droplet nuclei of sneezing, ★ breath generated aerosols. (a: $LoBF = \mathbf{1-7}$, b: Summation of deposited particles up to $LoBF = 7$)

Deposition, at 15 l/min steady state

breath generated particles

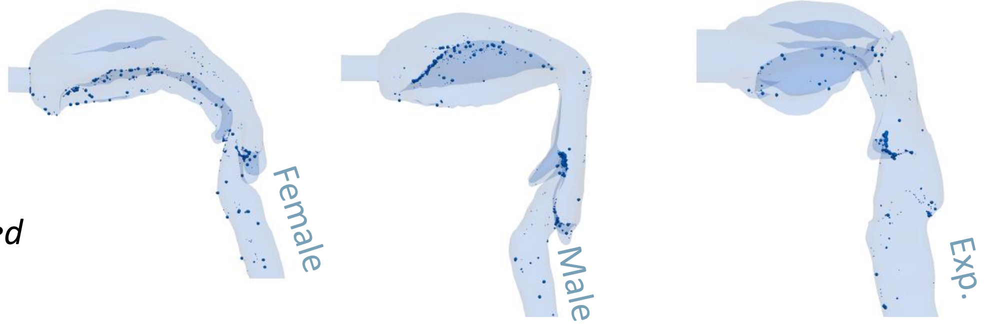

- Particles are colored according to particle size and scaled with diameter

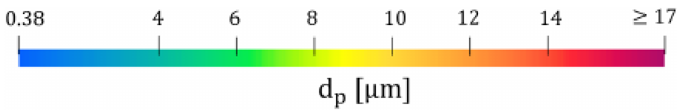

sneeze generated particles

cough generated particles

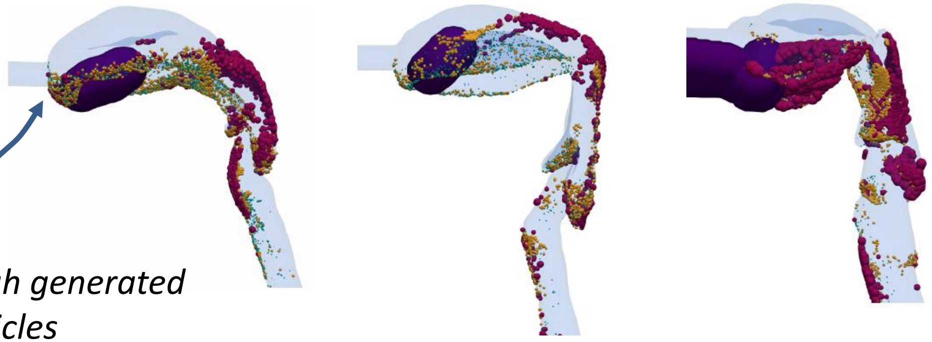

Deposition, 15 l/min, realistic inhalation

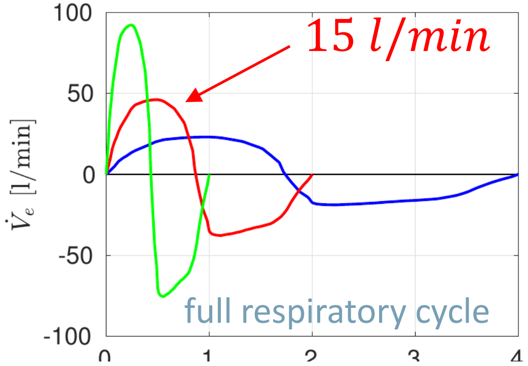

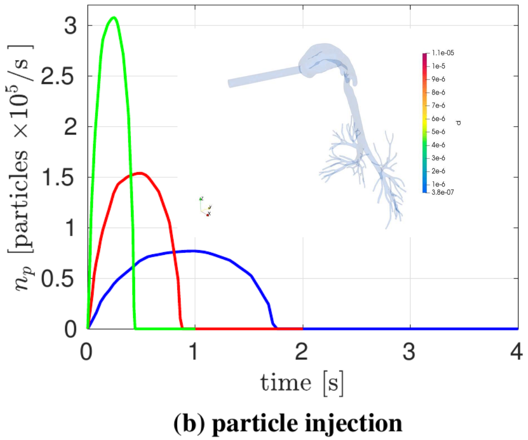

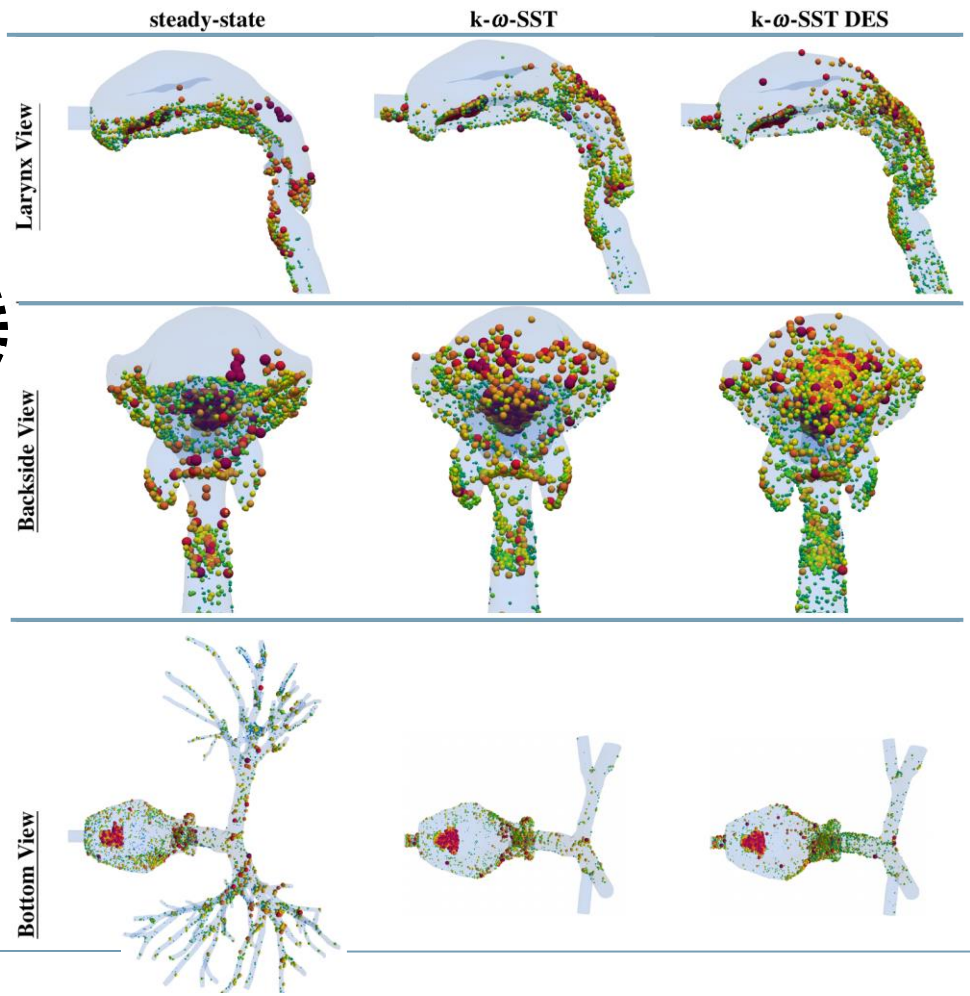

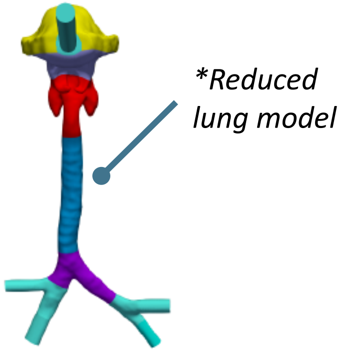

- Female lung
- $\dot{V}_e = 15\ l/min$
- sneeze generated particles

Room size and activity

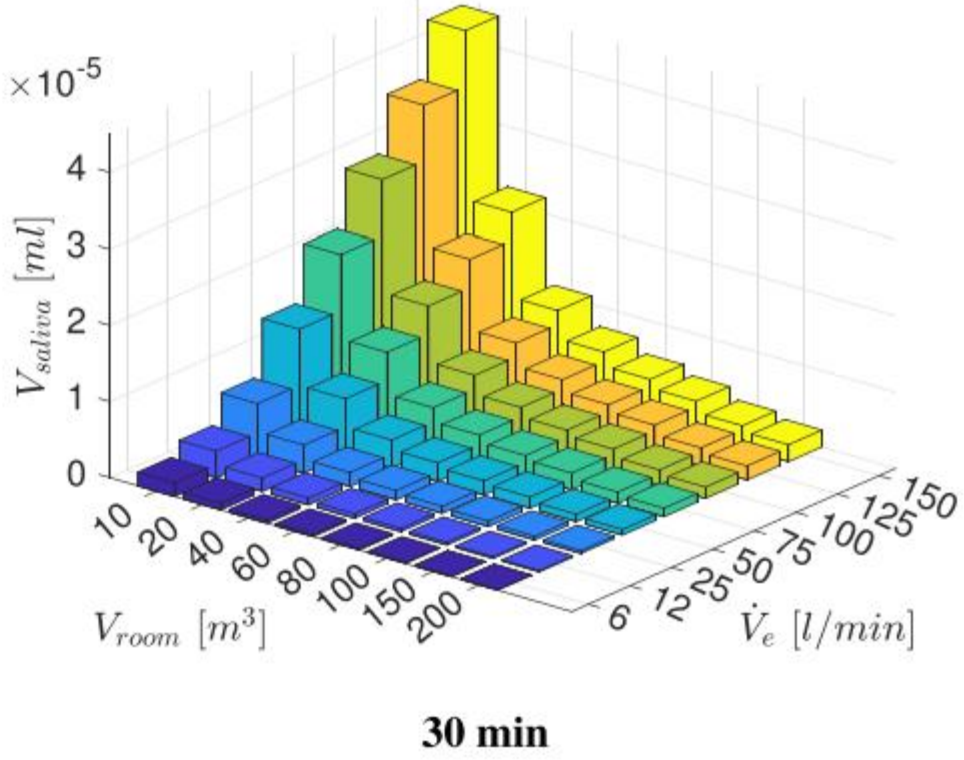

Fig. 10 Inhaled droplet/aerosol volume after a specified time

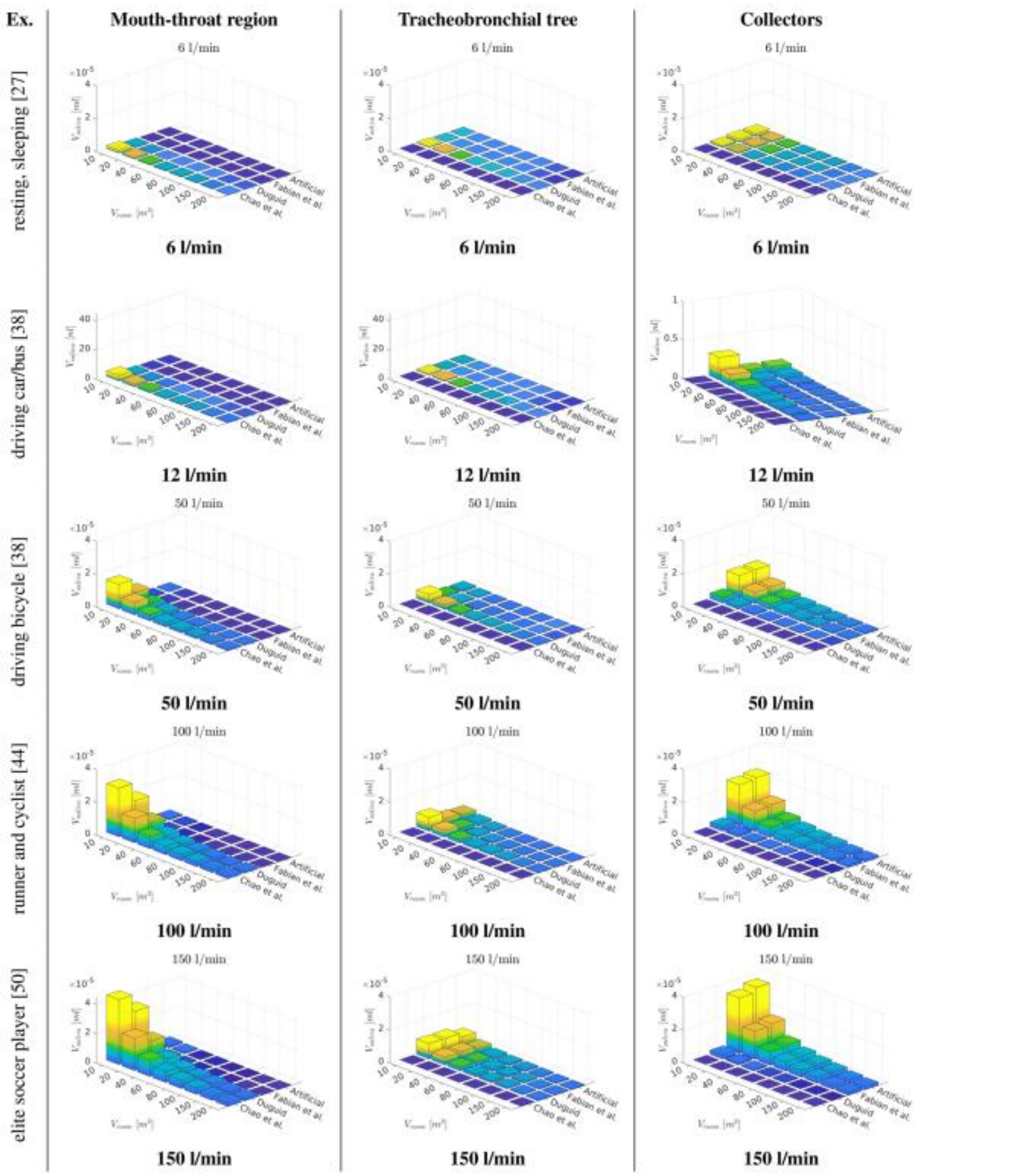

Fig. 11 Volumetric deposition of different particle size distributions across various exercising levels (Ex.) in varying room sizes (t_{inh} = 30 min)

Deposition in different lung sizes

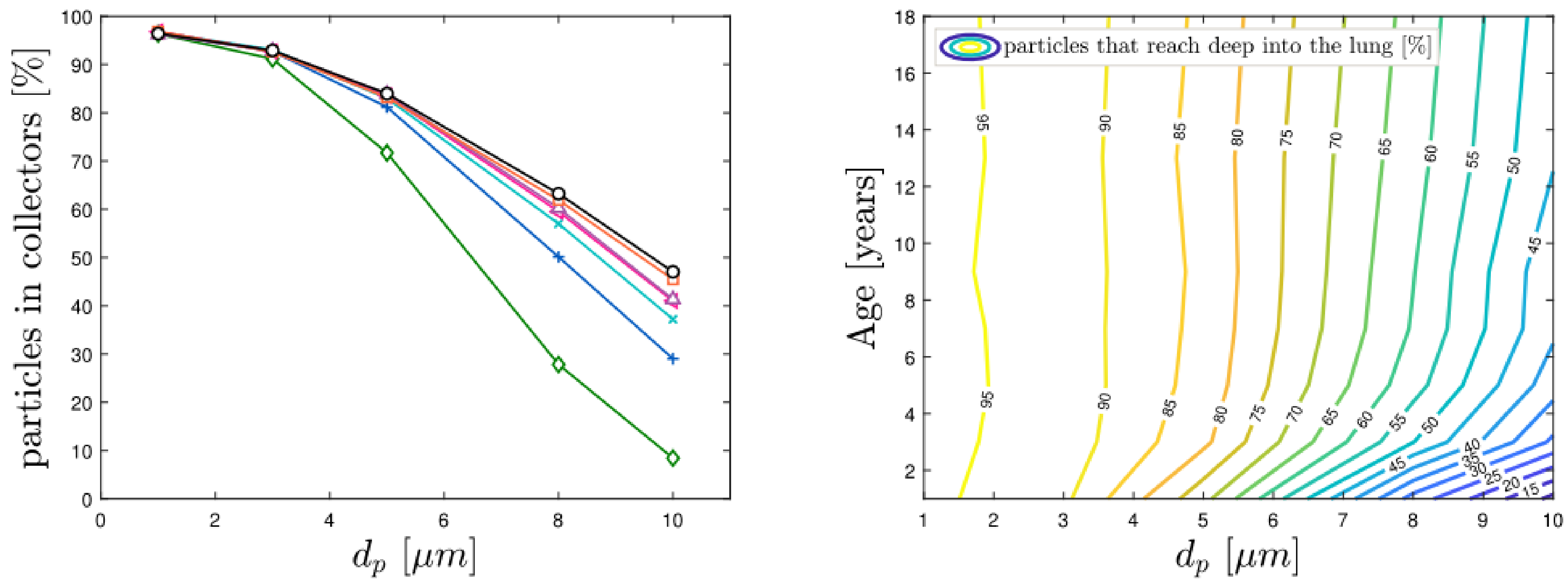

(d) Particles that reach deep into the lung

Fig. 7 Aerosol deposition for different lung sizes; ◇ Child (Age 1), + Child (Age 3), × Child (Age 5), ◁ Child (Age 7), △ Child (Age 9), □ Child (Age 13), ○ Adult (Male). (Color figure online)

Deposition in different lung sizes

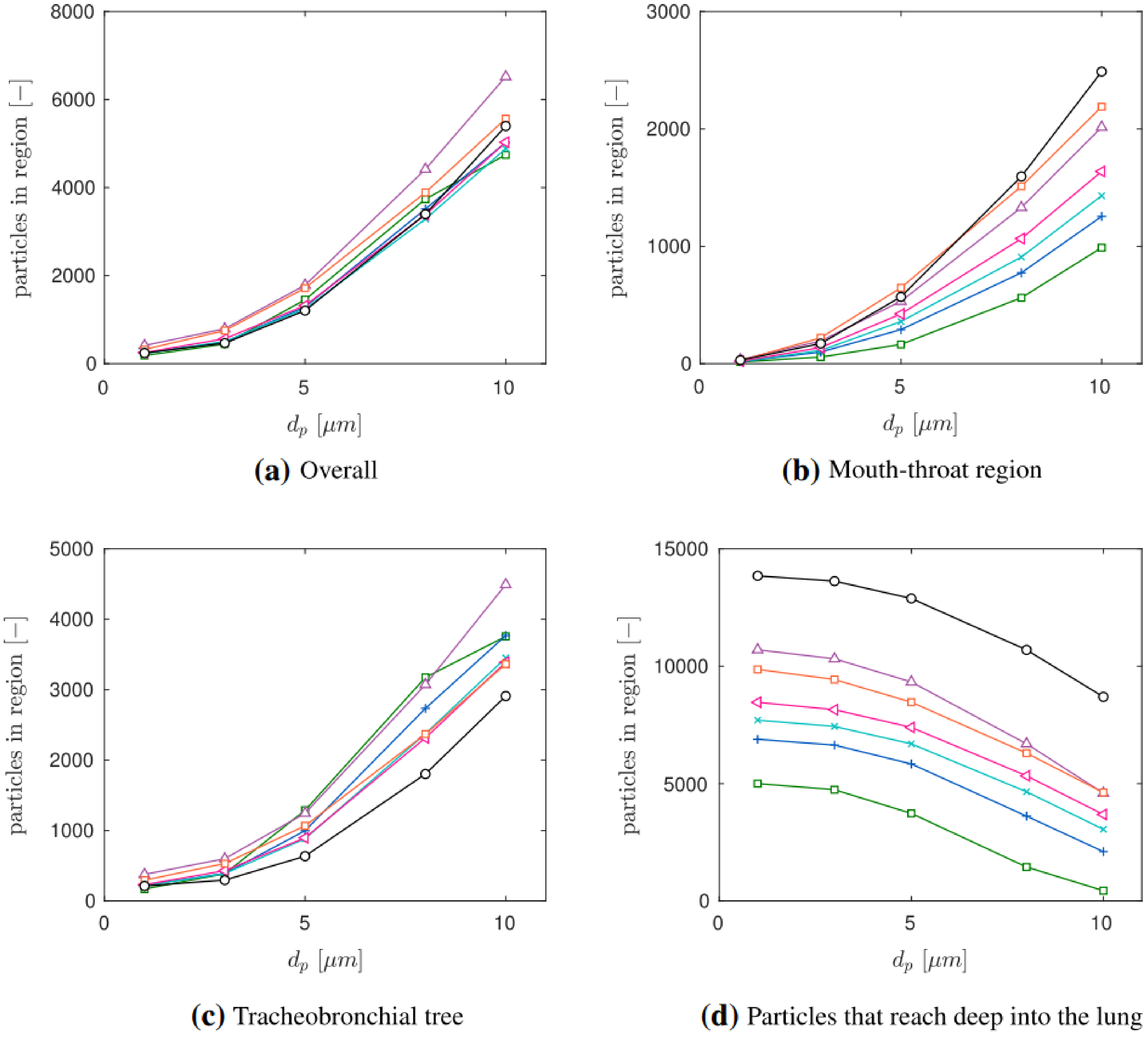

Fig. 11 Aerosol deposition after 15 *min*-inhalation for different lung sizes; ◇ Child (Age 1), + Child (Age 3), × Child (Age 5), ◁ Child (Age 7), △ Child (Age 9), □ Child (Age 13), ○ Adult (Male). (Color figure online)

FS Faculty

Tracking superellipsoid particles in flows

$$E(r') = \left[\left[\frac{x'}{a}\right]^{2/\epsilon_2} + \left[\frac{y'}{b}\right]^{2/\epsilon_2}\right]^{\epsilon_2/\epsilon_1} + \left[\frac{z'}{c}\right]^{2/\epsilon_1}$$

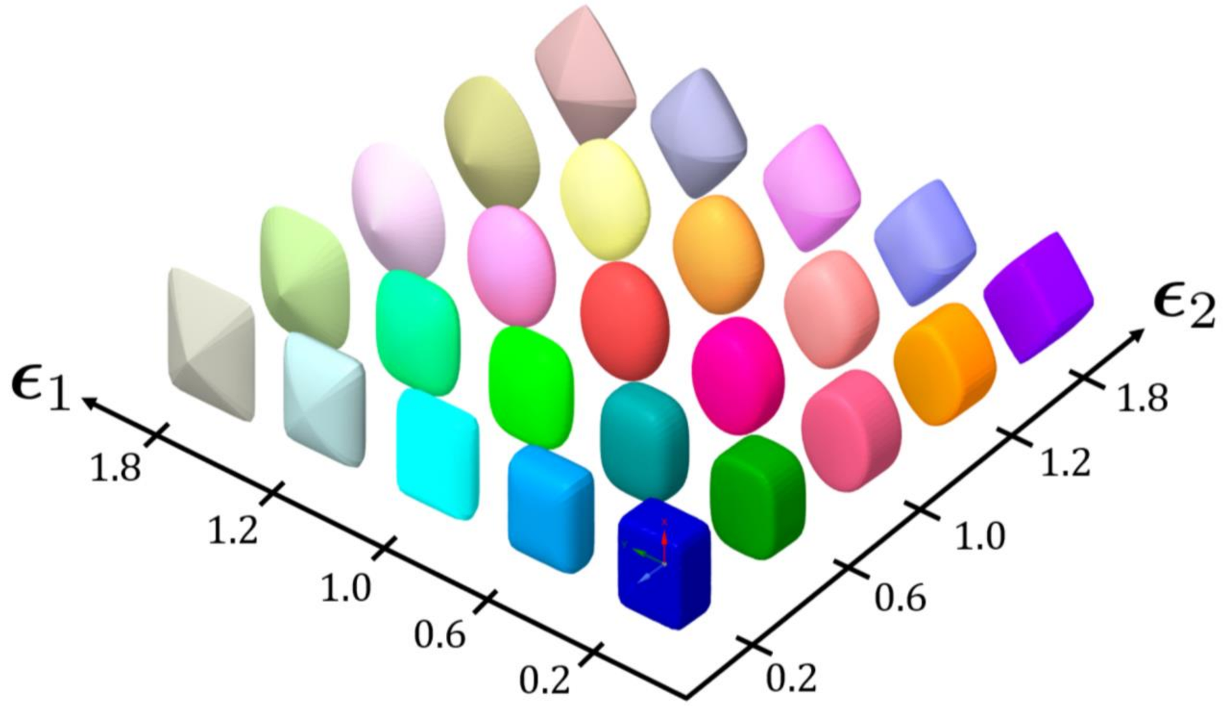

Particle-Fluid interaction models

- Drag & Torque acting on a particle
- Methods:
  - Analytical: direct integration from Stokes equations

Stokes flow form:

$\nabla \cdot \underline{\sigma} + \rho_f \vec{g} = 0$

Cauchy stress tensor:

$\underline{\sigma} = -P\underline{I} + \underline{\tau}$

<u>Drag:</u>

$$\vec{F} = \int_{\Gamma} \vec{\sigma} \cdot \vec{n} \, d\Gamma$$

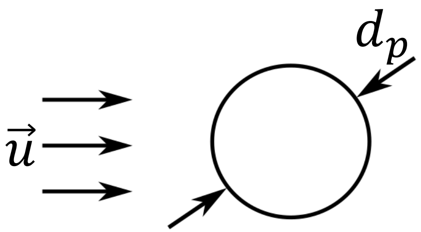

<u>Torque:</u>

$$\vec{T} = \int_{\Gamma} \vec{r} \times (\vec{\sigma} \cdot \vec{n}) \, d\Gamma$$

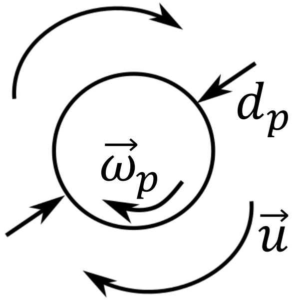

Spherical particle: $\vec{F} = 6\pi\mu d_p \cdot \vec{u}$ $\quad$ $\vec{T} = 8\pi\mu d_p^3 \cdot (\vec{\omega}_f - \vec{\omega}_p)$

Particle-Fluid interaction models

Prolate ellipsoid: $\vec{F} = \pi\,\mu c \underline{K} \cdot \vec{u}$ $\quad \vec{T} = \pi\,\mu c^3 \left[\underline{\Pi} \cdot \begin{bmatrix} f \\ g \\ h \end{bmatrix} + \underline{\Omega} \begin{bmatrix} \xi - \omega_x \\ \eta - \omega_y \\ \chi - \omega_z \end{bmatrix} \right]$

Drag:

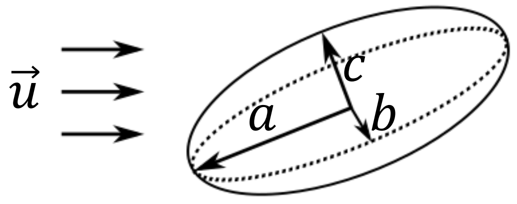

Translation resistance: $\underline{K}$

$$K_{xx} = \frac{8[\lambda_1^2 - 1]^{3/2}}{[2\lambda_1^2 - 1]\ln\left[\lambda_1 + \sqrt{\lambda_1^2 - 1}\right] - \lambda_1\sqrt{\lambda_1^2 - 1}}$$

$$K_{yy} = \mathrm{K}_{zz} = \frac{16[\lambda_1^2 - 1]^{3/2}}{[2\lambda_1^2 - 3]\ln\left[\lambda_1 + \sqrt{\lambda_1^2 - 1}\right] - \lambda_1\sqrt{\lambda_1^2 - 1}}$$

Shear:

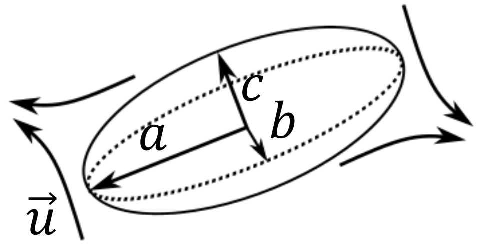

Deformation resistance: $\underline{\Pi}$

$$\Pi_{xx} = 0$$

$$\Pi_{zz} = -\Pi_{yy} = \frac{16\lambda_1}{3}\frac{1 - \lambda_1^2}{\alpha_0 + \lambda_1^2\gamma_0}$$

Spin:

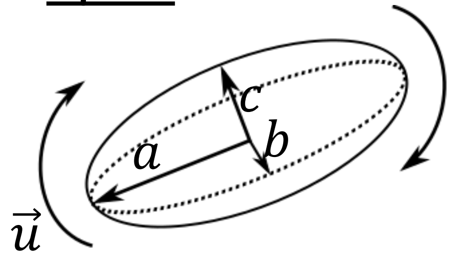

Rotation resistance: $\underline{\Omega}$

$$\Omega_{xx} = \frac{16\lambda_1}{3}\frac{1}{\alpha_0}$$

$$\Omega_{yy} = \Omega_{zz} = \frac{16\lambda_1}{3}\frac{1 + \lambda_1^2}{\alpha_0 + \lambda_1^2\gamma_0}$$

Particle-Fluid interaction models

- Methods:
  - Experimental
    - Sedimentation velocity in viscous fluids
    - Predominantely drag models
    - Lack of rotation prediction
  - Generalized shape description parameters:

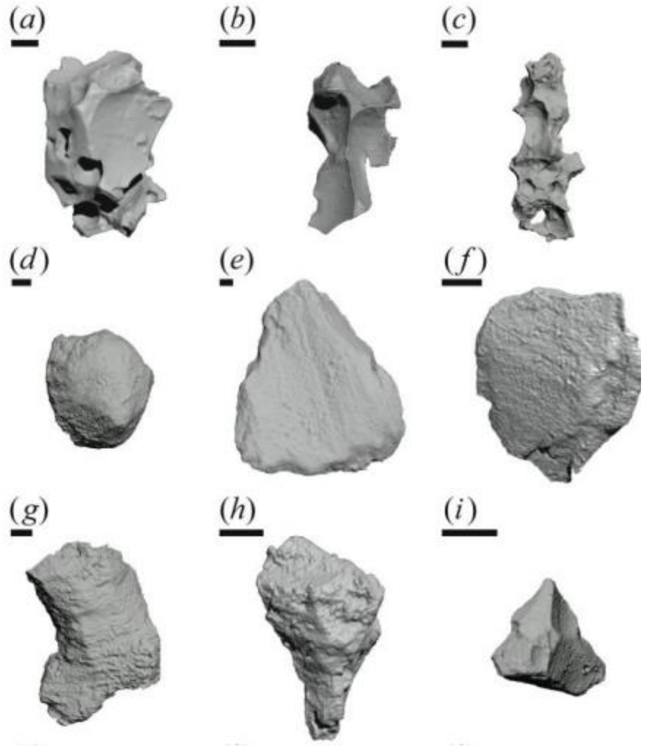

Aspect ratio:

$$A_R = \frac{d_{min}}{d_{max}}$$

Sphericity:

$$\Psi = \frac{A_s}{A_p} = \frac{\pi^{\frac{1}{3}}(6V_p)^{2/3}}{A_p}$$

Crosswise - sphericity:

$$\Psi_{\perp} = \frac{\sigma_s}{A_{p_{\perp}}} = \frac{\frac{1}{4}\pi^{\frac{1}{3}}(6V_p)^{2/3}}{A_{p_{\perp}}}$$

Lengthwise - sphericity:

$$\Phi_{\parallel} = \frac{\sigma_s}{\frac{1}{2}A_p - A_{p_{\parallel}}} = \frac{\frac{1}{4}\pi^{\frac{1}{3}}(6V_p)^{2/3}}{\frac{1}{2}A_p - A_{p_{\parallel}}}$$

Superellipsoid particle

- Parametric surface equation:

$$S(x,y,z) = \left(\left|\frac{x}{a}\right|^{2/e_2} + \left|\frac{y}{b}\right|^{2/e_2}\right)^{e_2/e_1} + \left|\frac{z}{c}\right|^{2/e_1}$$

- Superellipsoid volume:

$$V_p = 2abce_1e_2B\left(\frac{e_1}{2}+1, e_1\right)B\left(\frac{e_2}{2},\frac{e_2}{2}\right)$$

- Axial ratios

$$\lambda_1 = a/c$$

$$\lambda_2 = b/c$$

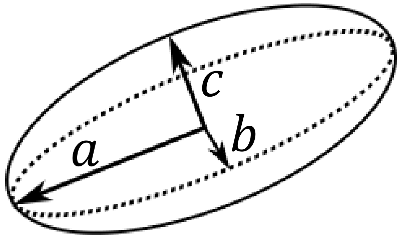

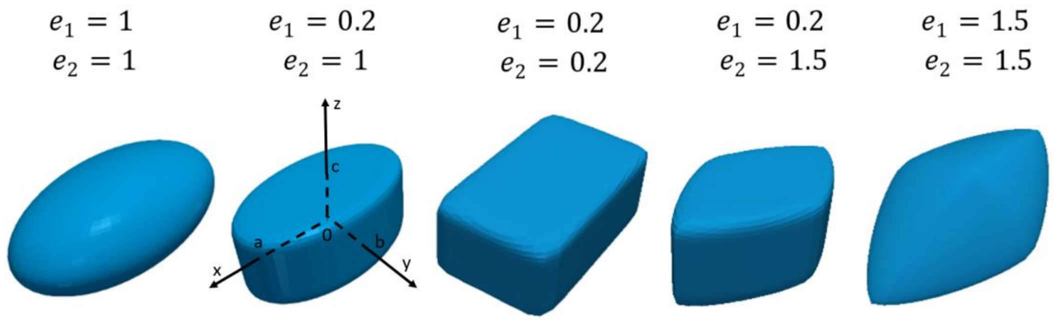

Normalized volume:

$$V_p = \frac{\pi}{6} \Rightarrow$$

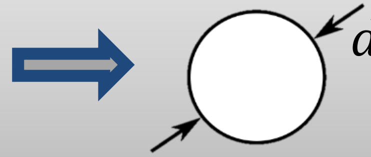

$$d_p = 1$$

$$c = \left[\frac{\pi}{\left[12\lambda_1\lambda_2e_1e_2B\left(\frac{e_1}{2}+1, e_1\right)B\left(\frac{e_2}{2},\frac{e_2}{2}\right)\right]}\right]^{1/3}$$

Reduced parameters: $\lambda_1, \lambda_2, e_1, e_2$

Design of numerical experiments

- Numerical approach
  - Parameter range: → ~5400 Particles
  - Superposition of simple flow fields
    - Investigated separately

$$\lambda_1 = [1,11] \qquad \lambda_2 \geq \lambda_1$$

$$e_1 = [0.2,1.8] \qquad e_2 = [0.2,1.8]$$

$$\vec{F} = \pi\, \mu c \underline{K} \cdot \vec{u}$$

$$\vec{T} = \pi\, \mu c^3 \left[\underline{\Pi} \cdot \begin{bmatrix} f \\ g \\ h \end{bmatrix} + \underline{\Omega} \begin{bmatrix} \xi - \omega_x \\ \eta - \omega_y \\ \chi - \omega_z \end{bmatrix} \right]$$

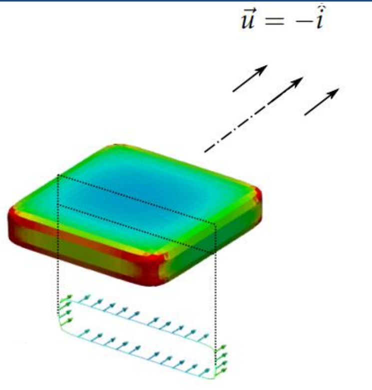

Translation

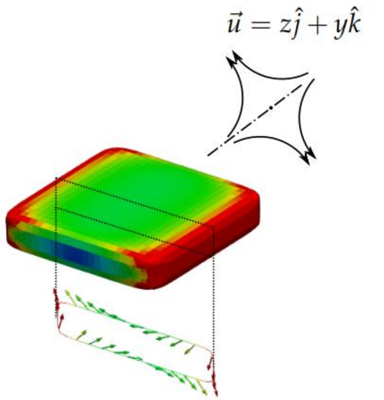

Shear

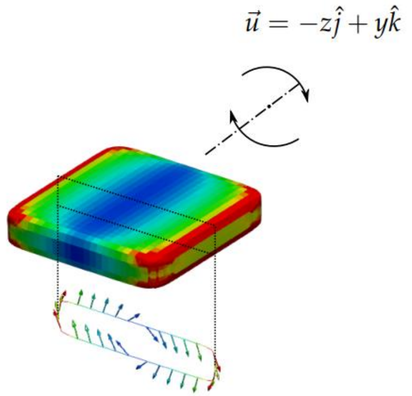

Rotation

Numerical framework

- Boundary element method
  - Spherical domain boundary
    - Constant velocity field
  - Domain size >> d_p
    - Momentum transport by diffusion
  - Particle in the domain centre
    - No slip condition
  - Particle force and torque

$$\vec{F} = \int_\Gamma \vec{\sigma} \cdot \vec{n} \, d\Gamma \qquad \vec{T} = \int_\Gamma \vec{r} \times (\vec{\sigma} \cdot \vec{n}) \, d\Gamma$$

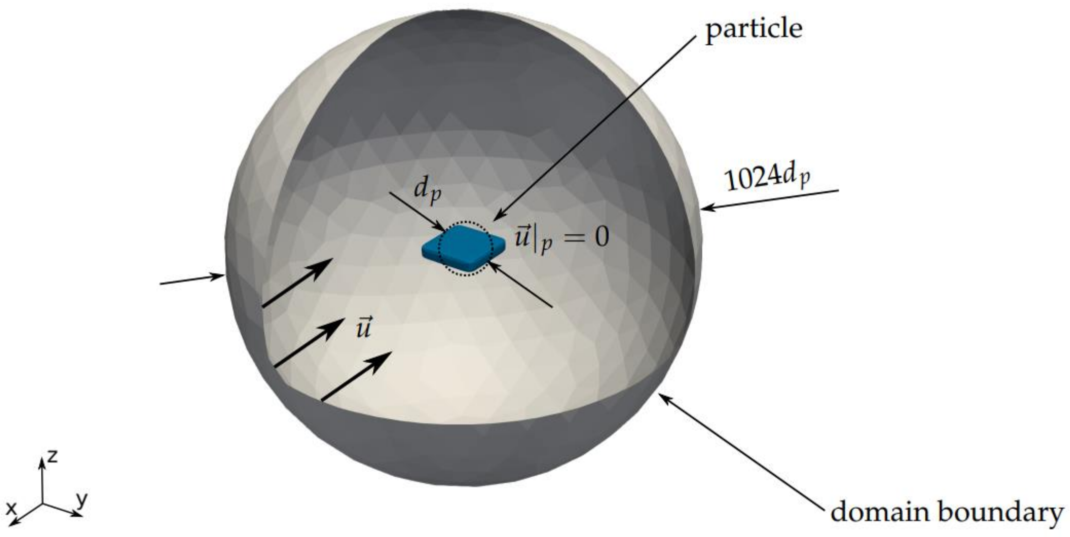

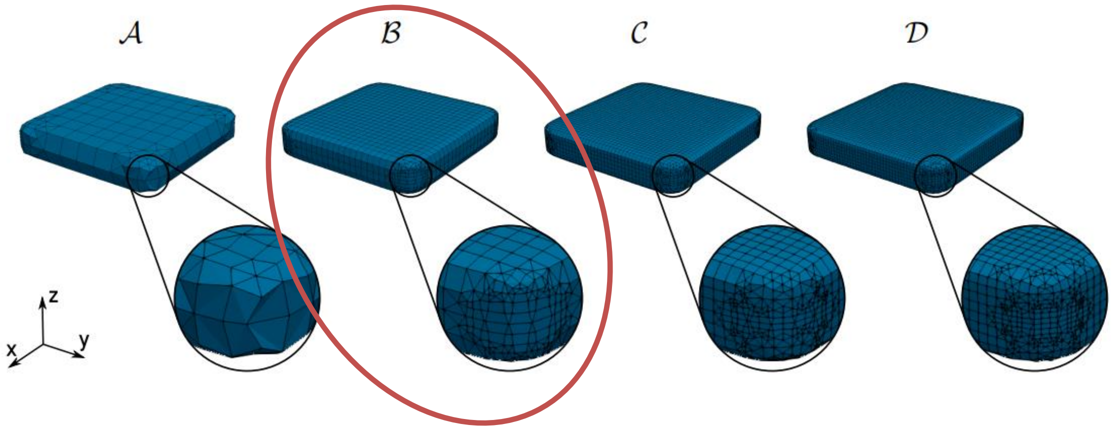

Convergent mesh

Numerical results

- Computed on 5400 intervals of $\lambda_1, \lambda_2, e_1, e_2$
  - 9 simulations per particle (3 flows × 3 directions)

$e_1, e_2 = 1$

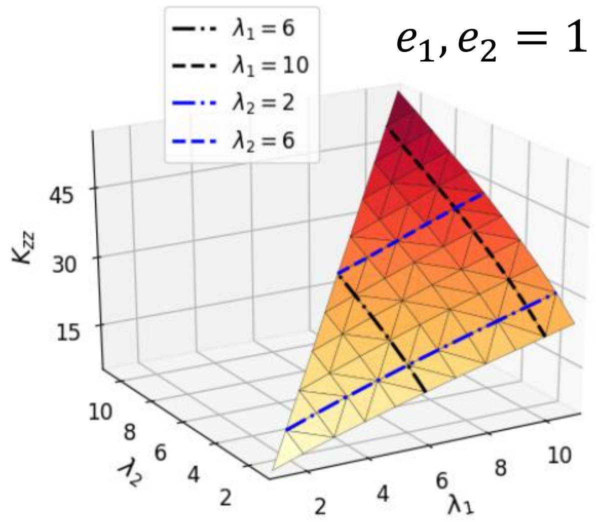

$\lambda_1, \lambda_2 = 5,3$

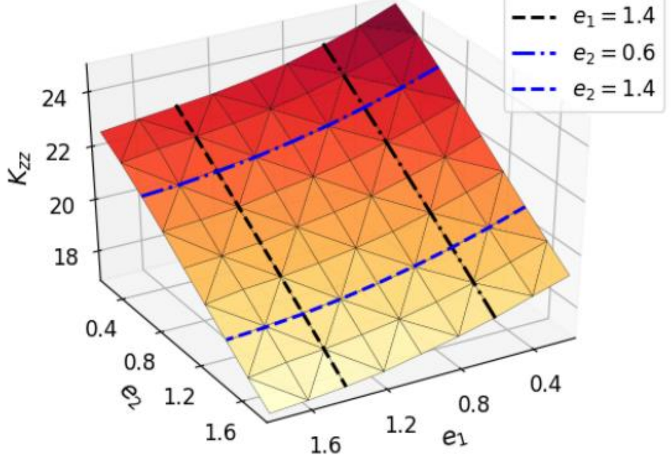

- Data representation
  - 4-dimensional space
  - Model derivation
    - For each individual tensor component via polynomial approximation

Force and torque model

Translation resistance tensor: (drag)

Particle [a]	Coeff. $\underline{K}$	An. Res.	Pres. BEM	Sphere	Prolate ell. [b]	[27]	[28]	[29]	Approx. Scheme
I. 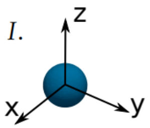	K_{xx}	6.0	6.002	6.0	6.0	6.046	5.845	5.871	6.003
	K_{yy}	6.0	6.002	6.0	6.0	6.046	5.894	5.876	6.003
	K_{zz}	6.0	6.002	6.0	6.0	6.046	5.845	5.854	6.004
		Average error:		0.0%	0.0%	0.44%	1.34%	1.28%	0.03%
II. 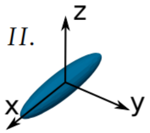	K_{xx}	10.71	10.69	6.0	10.71	10.54	9.728	11.16	10.70
	K_{yy}	14.23	14.22	6.0	14.23	10.54	12.23	12.03	14.23
	K_{zz}	14.23	14.22	6.0	14.23	10.54	12.12	11.97	14.24
		Average error:		30.95%	0.00%	11.04%	7.44%	7.17%	0.05%
III. 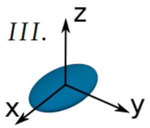	K_{xx}	–	15.50	6.0	10.71	15.24	14.73	16.39	15.50
	K_{yy}	–	17.07	6.0	14.23	15.24	15.82	16.62	17.06
	K_{zz}	–	20.56	6.0	14.23	15.24	18.87	18.40	20.57
		Average error:		37.91%	15.08%	8.00%	4.00%	3.78%	0.02%
IV. 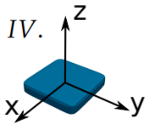	K_{xx}	–	24.73	6.0	10.71	22.37	22.18	25.27	24.83
	K_{yy}	–	24.73	6.0	14.23	22.37	22.22	25.29	24.82
	K_{zz}	–	30.92	6.0	14.23	22.37	27.97	28.25	30.98
		Average error:		44.54%	29.44%	9.48%	5.72%	2.69%	0.17%
V. 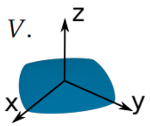	K_{xx}	–	32.33	6.0	15.88	29.76	30.00	35.39	32.40
	K_{yy}	–	32.31	6.0	22.87	29.76	30.41	35.43	32.35
	K_{zz}	–	45.87	6.0	22.87	29.76	42.16	41.44	45.98
		Average error:		47.62%	25.16%	10.93%	4.08%	5.47%	0.11%

Rotation resistance tensor: (spin)

Particle [a]	Coeff. $\underline{\Omega}$	An. Res.	Pres. BEM	Sphere	Prolate ell. [b]	Approx. Scheme
II. 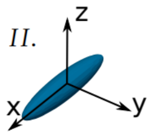	Ω_{xx}	28.24	27.76	8.0	28.24	27.91
	Ω_{yy}	185.6	184.4	8.0	185.6	185.2
	Ω_{zz}	185.6	184.2	8.0	185.6	185.0
		Average error:		47.41%	0.0%	0.19%
IV. 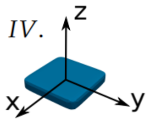	Ω_{xx}	–	782.0	8.0	28.24	784.5
	Ω_{yy}	–	782.0	8.0	185.6	784.0
	Ω_{zz}	–	1023	8.0	185.6	1025
		Average error:		56.71%	48.40%	0.14%

Deformation resistance tensor: (shear)

Particle [a]	Coeff. $\underline{\Pi}$	An. Res.	Pres. BEM	Sphere	Prolate ell. [b]	Approx. Scheme
II. 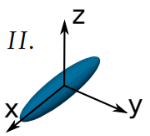	Π_{xx}	0.0	0.021	0.0	0.0	0.021
	Π_{yy}	−171.3	−170.4	0.0	−171.3	−171.1
	Π_{zz}	171.3	170.2	0.0	171.3	170.8
		Average error:		47.14%	0.0%	0.11%
IV. 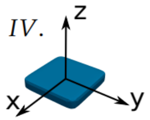	Π_{xx}	–	672.9	0.0	0.0	676.1
	Π_{yy}	–	−671.9	0.0	−171.3	−675.2
	Π_{zz}	–	−0.083	0.0	171.3	−0.006
		Average error:		47.14%	47.14%	0.23%

Force and torque model

- Reallistic pollen particle
  - Reconstruct 3D geometry
  - Find best fitting superellipsoid
- Optimization problem:

$$\min_{\lambda_1,\lambda_2,e_1,e_2} \sum_{i=1}^{n} [S(x_i, y_i, z_i) - 1]^2$$

$\lambda_1 = 1.96$, $\lambda_2 = 1.83$,
$e_1 = 0.564$, $e_2 = 0.472$;

3D surface points

Superellipsoid surface:

$$S(x,y,z) = \left(\left| \frac{x}{\lambda_1 c} \right|^{2/e_2} + \left| \frac{y}{\lambda_2 c} \right|^{2/e_2} \right)^{e_2/e_1} + \left| \frac{z}{c} \right|^{2/e_1}$$

Particle image | 3D reconstruction | Fitted superellipsoid

Coeff. K, Ω, Π	Pres. BEM	Sphere	Prolate ell. [b]	[27]	[28]	[29]	Approx. Scheme
K_{xx}	10.77	6.0	7.174	9.505	9.324	9.922	10.58
K_{yy}	10.80	6.0	8.184	9.505	9.431	9.968	10.71
K_{zz}	12.01	6.0	8.184	9.505	10.36	10.46	11.86
Average error:		26.76%	17.24%	8.70%	7.68%	5.56%	0.74%
Ω_{xx}	50.07	8.0	12.70	–	–	–	47.23
Ω_{yy}	50.88	8.0	23.14	–	–	–	50.71
Ω_{zz}	63.20	8.0	23.14	–	–	–	61.65
Average error:		49.00%	36.77%	–	–	–	1.60%
Π_{xx}	25.31	0.0	0.0	–	–	–	23.51
Π_{yy}	−26.22	0.0	−13.57	–	–	–	−27.56
Π_{zz}	0.86	0.0	13.57	–	–	–	3.791
Average error:		47.90%	46.34%	–	–	–	2.36%

A Model for Translation and Rotation Resistance Tensors for Superellipsoidal Particles

A model was developed that

- for a chosen **superellipsoid** with known **velocity** and **angular velocity**

at a location in the flow where

- the **flow velocity** and flow **velocity gradient** tensor are known

gives

- the **force** and **torque** on the particle

The model is available at Github:
https://github.com/transport-phenomena/superellipsoid-force-torque-model

Model used for a pollen particle

Table 3

K′, **Ω′** and **Π′** tensor coefficients estimations for a realistic pollen particle (Štrakl et al., 2022a), obtained via DNS, approximated via sphere, prolate ellipsoid, triaxial ellipsoid and superellipsoid.

K′, **Ω′**, **Π′**	Pollen[a] (Štrakl et al., 2022a)	Sphere[b]	Prolate[c]	Triaxial[d]	Superel.[e]	Shape factors		
		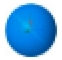		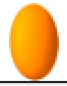		Haider and Levenspiel (1989)	Leith (1987)	Hölzer and Sommerfeld (2008)
Case ID	–	A	B	C	D1/D2	E1/E2	F1/F2	G1/G2
K'_{xx}	10.7	6	7.235	9.413	10.58	9.505	9.324	9.922
K'_{yy}	10.80	6	8.293	9.582	10.71	9.505	9.431	9.968
K'_{zz}	12.01	6	8.293	10.84	11.86	9.505	10.36	10.46
Ω'_{xx}	50.07	8	12.95	34.05	0/47.23	0/8	0/8	0/8
Ω'_{yy}	50.88	8	24.29	37.65	0/50.71	0/8	0/8	0/8
Ω'_{zz}	63.20	8	24.29	44.79	0/61.65	0/8	0/8	0/8
Π'_{xx}	25.31	0	0.0	19.35	0/23.51	0/0	0/0	0/0
Π'_{yy}	−26.22	0	−14.63	−23.53	0/−27.56	0/0	0/0	0/0
Π'_{zz}	0.86	0	14.63	3.87	0/3.791	0/0	0/0	0/0
$K'_{xx}2c/d_{eq}$	6.09	6	5.733	5.944	0/6.025	5.412	5.309	5.650
$K'_{yy}2c/d_{eq}$	6.15	6	6.572	6.051	0/6.100	5.412	5.370	5.676
$K'_{zz}2c/d_{eq}$	6.84	6	6.572	6.846	0/6.756	5.412	5.899	5.956

[a] Fitted tensor coefficients (Štrakl et al., 2022a) solely for comparison (superellipsoid surrogate approach not applicable due to non-symmetric particle shape).

[b] Analytical tensor coefficients for $\lambda_1 = \lambda_2 = \epsilon_1 = \epsilon_2 = 1.0$.

[c] Analytical tensor coefficients for $\lambda_1 = 2.009;\ \lambda_2 = \epsilon_1 = \epsilon_2 = 1.0$.

[d] Superellipsoid surrogate mode, l (Štrakl et al., 2022a), for $\lambda_1 = 2.081;\ \lambda_2 = 1.907;\ \epsilon_1 = \epsilon_2 = 1.0$.

[e] Superellipsoid surrogate approach, Štrakl et al. (2022a), for $\lambda_1 = 1.96;\ \lambda_2 = 1.83;\ \epsilon_1 = 0.564;\ \epsilon_2 = 0.472$.

A pollen particle in laminar pipe flow

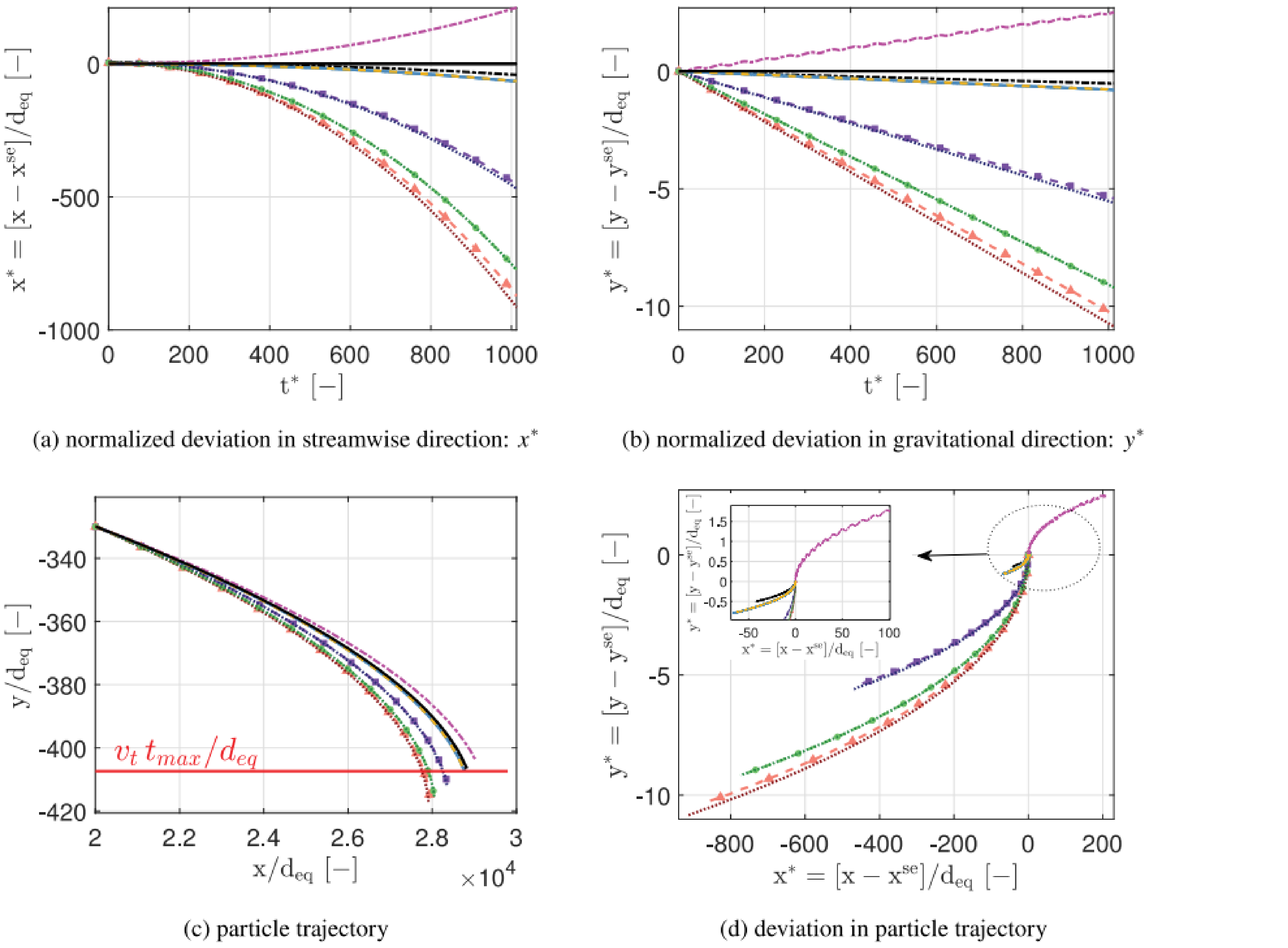

Fig. 11. Deviation of particle position compared to superellipsoid particle position (x^{se}, y^{se}). The deviation is normalized to the volume equivalent diameter of a sphere (d_{eq}). The intial particle orientation is set to $\varphi = -90°$, $\theta = 0°$, $\psi = 0°$. A, B, C, D2, D1, E1, F1, G1, E2, F2, G2, maximal descent of a settling sphere in Stokes flow ($y_{max}/d_{eq} = v_t\ t_{max}/d_{eq}$).

Superellipsoid collision modelling

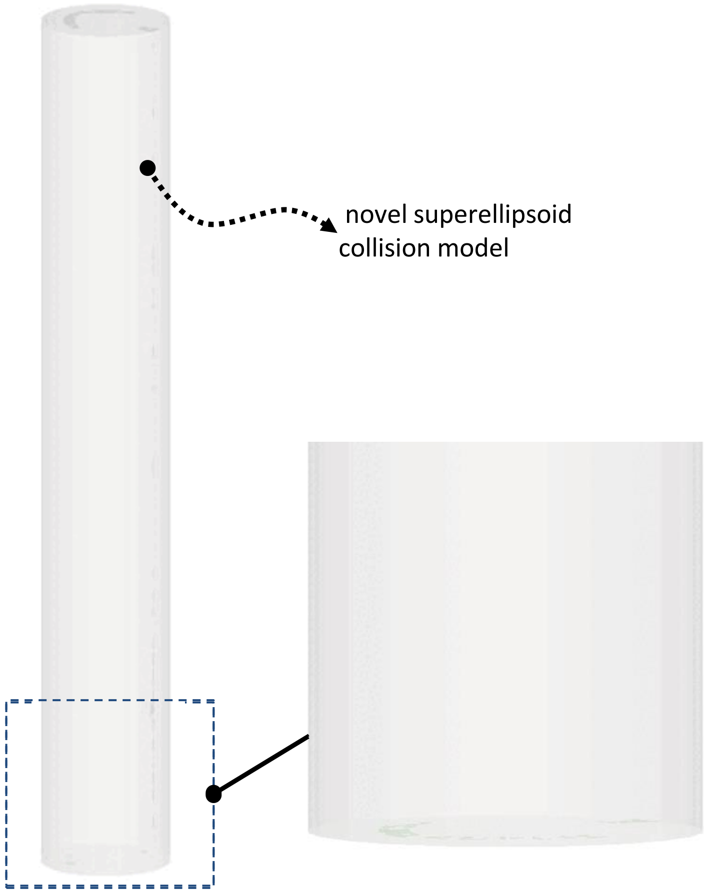

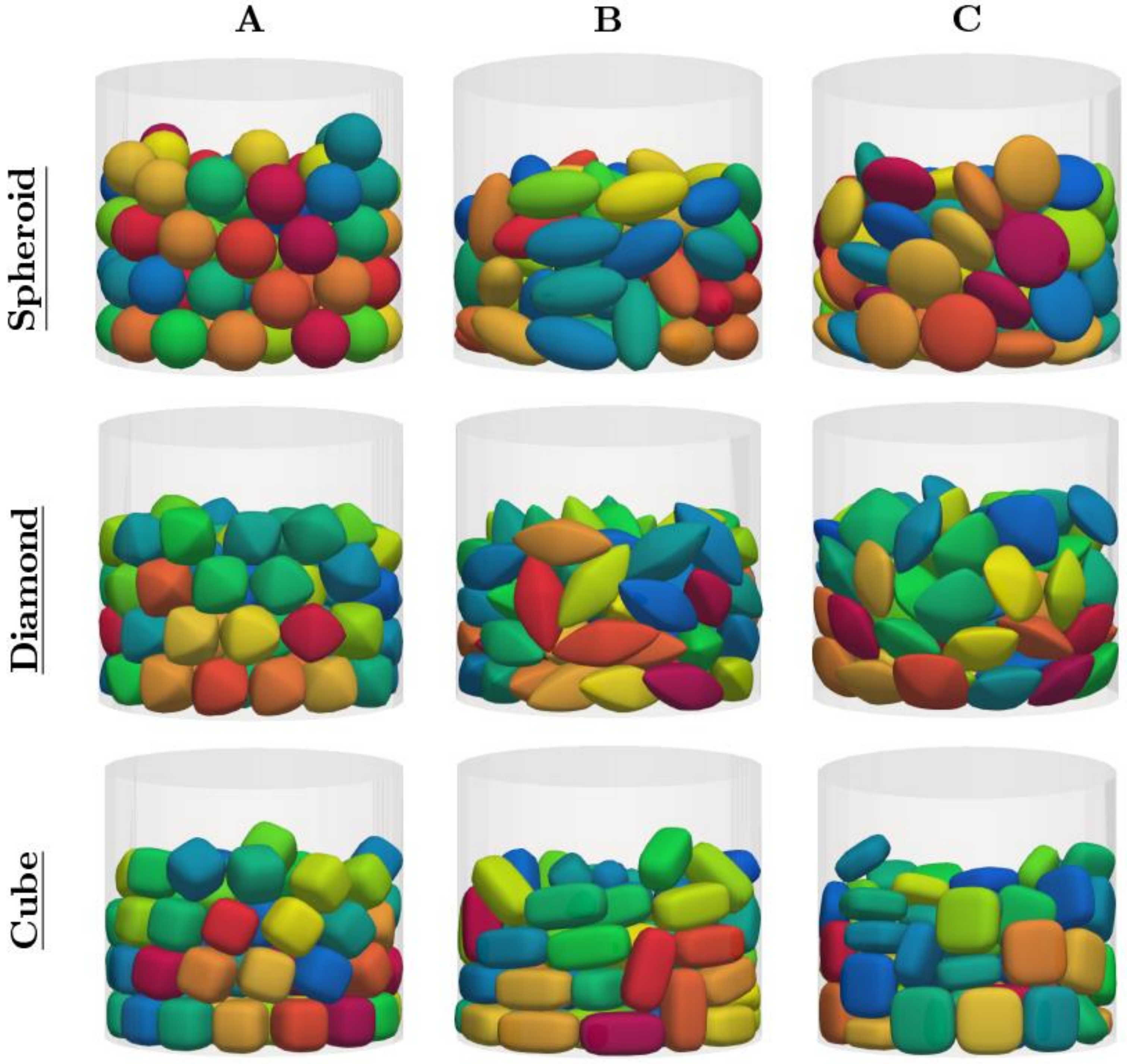

Detect contact point

- A point on the surface of one superellipsoid is inside of the second superellipsoid.
- We solve an optimization problem that seeks the point on the second superellipsoid that is deepest inside of the first.

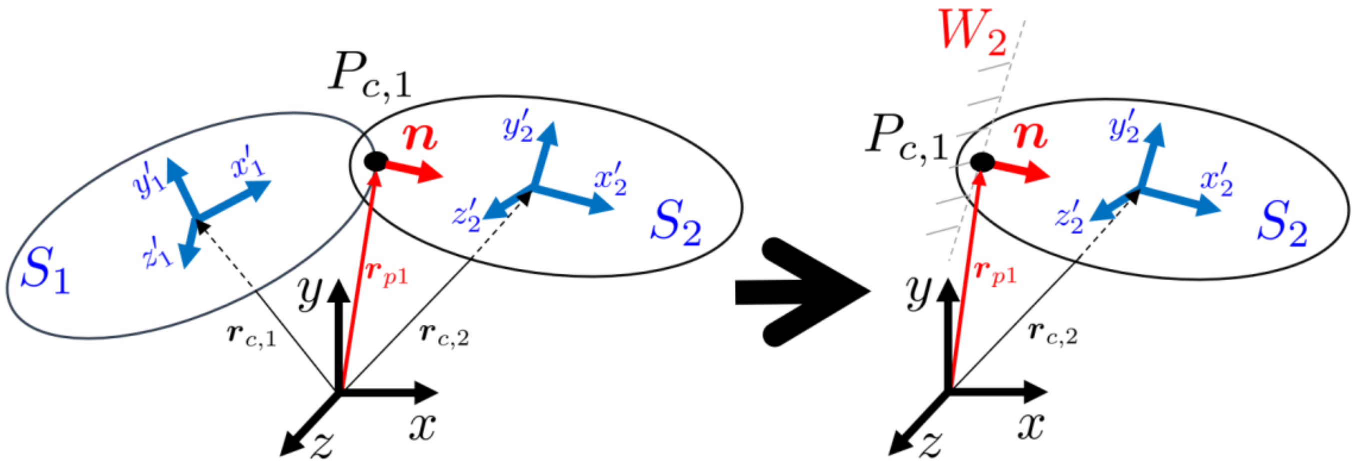

Figure 8: Detection of collision point on superellipsoid 2 and inside superellipsoid 1 with common normal $\boldsymbol{n}$

Collision model

- We assume the particles are rigid with elastic contact (coef. of restitution normal direction < 1)
- Friction is modelled by tangential coef. of restitution (-1,1)
- Conservation of linear and angular momentum are considered.

$$\underline{b} = \begin{bmatrix} m_1 v''_{1x} + m_2 v''_{2x} \\ m_1 v''_{1y} + m_2 v''_{2y} \\ m_1 v''_{1z} + m_2 v''_{2z} \\ -\epsilon_n \left[v_{2x} - \omega_{2y} r_{2z} + \omega_{2z} r_{2y} - v_{1x} + \omega_{1y} r_{1z} - \omega_{1z} r_{1y} \right] \\ \epsilon_t \left[v_{2y} - \omega_{2z} r_{2x} + \omega_{2x} r_{2z} - v_{1y} + \omega_{1z} r_{1x} - \omega_{1x} r_{1z} \right] \\ \epsilon_t \left[v_{2z} - \omega_{2x} r_{2y} + \omega_{2y} r_{2x} - v_{1z} + \omega_{1x} r_{1y} - \omega_{1y} r_{1x} \right] \\ I''_{1xx}\omega''_{1x} + I''_{1xy}\omega''_{1y} + I''_{1xz}\omega''_{1z} + m_1 r''_{1y} v''_{1z} - m_1 r''_{1z} v''_{1y} \\ I''_{1yx}\omega''_{1x} + I''_{1yy}\omega''_{1y} + I''_{1yz}\omega''_{1z} + m_1 r''_{1z} v''_{1x} - m_1 r''_{1x} v''_{1z} \\ I''_{1zx}\omega''_{1x} + I''_{1zy}\omega''_{1y} + I''_{1zz}\omega''_{1z} + m_1 r''_{1x} v''_{1y} - m_1 r''_{1y} v''_{1x} \\ I''_{2xx}\omega''_{2x} + I''_{2xy}\omega''_{2y} + I''_{2xz}\omega''_{2z} + m_2 r''_{2y} v''_{2z} - m_2 r''_{2z} v''_{2y} \\ I''_{2yx}\omega''_{2x} + I''_{2yy}\omega''_{2y} + I''_{2yz}\omega''_{2z} + m_2 r''_{2z} v''_{2x} - m_2 r''_{2x} v''_{2z} \\ I''_{2zx}\omega''_{2x} + I''_{2zy}\omega''_{2y} + I''_{2zz}\omega''_{2z} + m_2 r''_{2x} v''_{2y} - m_2 r''_{2y} v''_{2x} \end{bmatrix}$$

$$\underline{A} = \begin{bmatrix} m_1 & 0 & 0 & m_2 & 0 & 0 & 0 & 0 & 0 & 0 & 0 & 0 \\ 0 & m_1 & 0 & 0 & m_2 & 0 & 0 & 0 & 0 & 0 & 0 & 0 \\ 0 & 0 & m_1 & 0 & 0 & m_2 & 0 & 0 & 0 & 0 & 0 & 0 \\ -1 & 0 & 0 & 1 & 0 & 0 & 0 & r''_{1z} & -r''_{1y} & 0 & -r''_{2z} & r''_{2y} \\ 0 & -1 & 0 & 0 & 1 & 0 & -r''_{1z} & 0 & r''_{1x} & r''_{2z} & 0 & -r''_{2x} \\ 0 & 0 & -1 & 0 & 0 & 1 & r''_{1y} & -r''_{1x} & 0 & -r''_{2y} & r''_{2x} & 0 \\ 0 & -m_1 r''_{1z} & m_1 r''_{1y} & 0 & 0 & 0 & I''_{xx} & I''_{xy} & I''_{xz} & 0 & 0 & 0 \\ m_1 r''_{1z} & 0 & -m_1 r''_{1x} & 0 & 0 & 0 & I''_{yx} & I''_{yy} & I''_{yz} & 0 & 0 & 0 \\ -m_1 r''_{1y} & m_1 r''_{1x} & 0 & 0 & 0 & 0 & I''_{zx} & I''_{zy} & I''_{zz} & 0 & 0 & 0 \\ 0 & 0 & 0 & 0 & -m_2 r''_{2z} & m_2 r''_{2y} & 0 & 0 & 0 & I''_{xx} & I''_{xy} & I''_{xz} \\ 0 & 0 & 0 & m_2 r''_{2z} & 0 & -m_2 r''_{2x} & 0 & 0 & 0 & I''_{yx} & I''_{yy} & I''_{yz} \\ 0 & 0 & 0 & -m_2 r''_{2y} & m_2 r''_{2x} & 0 & 0 & 0 & 0 & I''_{zx} & I''_{zy} & I''_{zz} \end{bmatrix}$$

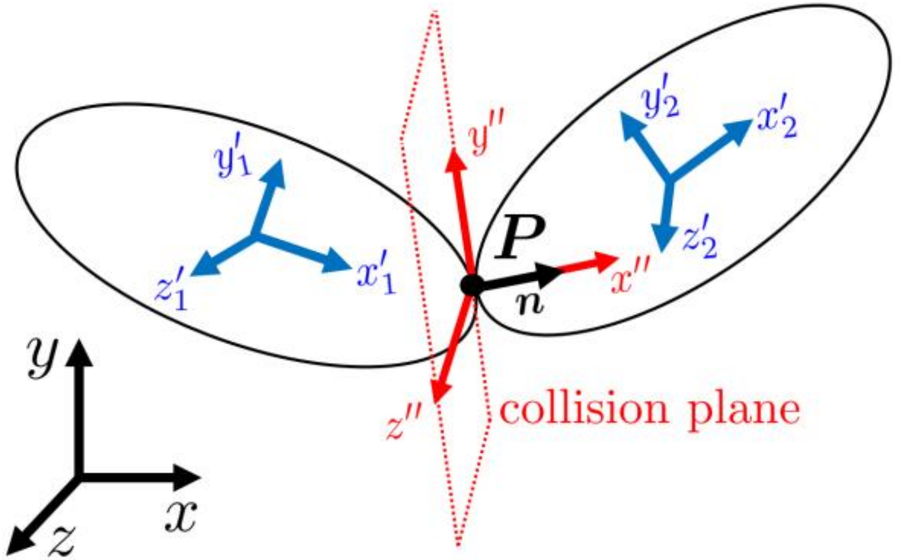

Figure 10: Two superellipsoidal particles undergoing collision

Faculty of Mechanical Engineering

Thank you for your attention!

dr. Jure Ravnik,

professor of power, process and environmental engineering

References:

- Wedel, J., Steinmann, P., Štrakl, M., Hriberšek, M., & Ravnik, J. (2023). Shape matters**: Lagrangian tracking of complex nonspherical microparticles in superellipsoidal approximation**. International Journal of Multiphase Flow, 158, 104283. doi:10.1016/j.ijmultiphaseflow.2022.104283
- Wedel, J., Steinmann, P., Štrakl, M., Hriberšek, M., Cui, Y., & Ravnik, J. (2022). **Anatomy matters: The role of the subject-specific respiratory tract on aerosol deposition — A CFD study**. Computer Methods in Applied Mechanics and Engineering, 401, 115372. doi:10.1016/j.cma.2022.115372
- Štrakl, M., Hriberšek, M., Wedel, J., Steinmann, P., Ravnik, J. (2022**). A Model for Translation and Rotation Resistance Tensors for Superellipsoidal Particles in Stokes Flow**. J. Mar. Sci. Eng. 2022, 10, 369. doi:10.3390/jmse10030369
- Mitja Štrakl, Jana Wedel, Paul Steinmann, Matjaž Hriberšek & Jure Ravnik (2022). **Numerical drag and lift prediction framework for superellipsoidal particles in multiphase flows**. International Journal of Computational Methods and Experimental Measurements (2022), Vol 10, Pages 38-49, doi:10.1016/10.2495/CMEM-V10-N1-38-49
- J. Wedel, P. Steinmann, M. Štrakl, M. Hriberšek, J. Ravnik (2021). **Risk Assessment of Infection by Airborne Droplets and Aerosols at Different Levels of Cardiovascular Activity**. Archives of Computational Methods in Engineering (2021), doi:10.1007/s11831-021-09613-7
- J. Wedel, P. Steinmann, M. Štrakl, M. Hriberšek, J. Ravnik (2021**). Can CFD establish a connection to a milder COVID-19 disease in younger people? Aerosol deposition in lungs of different age groups based on Lagrangian particle tracking in turbulent flow**. Computational Mechanics, doi:10.1007/s00466-021-01988-5

Contact:

- ***jure.ravnik@um.si***
- ***http://jure.ravnik.si***
- ***@JureRavnik***

University of Maribor